Review

Roles of Organic Fragments in Redirecting Crystal/Molecular Structures of Inorganic–Organic Hybrids Based on Lacunary Keggin-Type Polyoxometalates

Ruhollah Khajavian [1], Vida Jodaian [2,*], Fatemeh Taghipour [1], Joel T. Mague [3] and Masoud Mirzaei [1,*]

[1] Department of Chemistry, Faculty of Science, Ferdowsi University of Mashhad, Mashhad 9177948974, Iran; ruhollah_khajavian2002@yahoo.com (R.K.); fatemetaghipoor@gmail.com (F.T.)

[2] Department of Chemistry, Islamshahr Branch, Islamic Azad University, Islamshahr 3317843154, Iran

[3] Department of Chemistry, Tulane University, New Orleans, LA 70118, USA; joelt@tulane.edu

[*] Correspondence: hvidajodaian@yahoo.co.nz (V.J.); mirzaeesh@um.ac.ir (M.M.); Tel.: +98-513-880-5554 (M.M.)

Abstract: Lacunary polyoxometalates (LPOMs) are key precursors for the synthesis of functional POMs. To date, reviews dedicated to behavioral studies of LPOMs often comprise the role of metal ions, including transition metal (TM) and rare earth (RE) ions, in extending and stability of high-nuclearity clusters. In contrast, the role of organic ligands in the structures and properties of lacunary-based hybrids has remained less explored. In this review, we focus on the role of organic fragments in the self-assembling process of POM-based architectures and discuss relationships between the nature and structure of organic ligand and properties such as the topology of hybrid inorganic–organic material in RE and TM-RE heterometallic derivatives of lacunary Keggin-type POMs. The effects of organic fragment in mixed ligand hybrids are also briefly reviewed.

1. Introduction

Polyoxometalates (POMs), a large group of fascinating polynuclear metal-oxo clusters of early transition metals such as Mo, W and V, constitute a marvelous class of inorganic systems, due to their intriguing structures and remarkable potential applications in electrochemistry, catalysis, magnetism, and medicine [1–6]. Lacunary POMs (LPOMs) with a set of remarkable properties such as high coordination reactivity, rigidity, oxidative and thermal stability are an important sub-class of POMs [7]. Typically, LPOMs imply that topologies gain by the loss of one single {MO} moiety or multiple $\{M_xO_{2x}\}$ moieties, resulting in the formation of the monolacunary or polylacunary POMs, respectively. Mainly, lacunary species are limited to polyoxotungstates, while lacunary POMs of polyoxomolybdates and polyoxovanadates are uncommon [8]. Tungsten skeleton of the POMs with saturated Keggin $[XW_{12}O_{40}]^{n-}$ and Wells–Dawson-type $[X_2W_{18}O_{62}]^{n-}$ structures can be partially decomposed by the addition of a weak base, while retaining the original Keggin- and Wells–Dawson-type structures, to form lacunary species, such as $[XW_{11}O_{39}]^{n-}$ and $[X_2W_{17}O_{61}]^{n-}$ [9]. The lacunary species with high negative charge and nucleophilic oxygen-enriched surfaces can interact with various cations. In fact, owing to the negative-charged surface and defect binding sites, LPOMs can act as outstanding multidentate nucleophilic ligands toward the electrophilic center. Transition metal (TM) or lanthanoide (Ln) cations can be incorporated into the defect sites of LPOMs to form metal-substituted POMs, which exhibit unique chemical properties that depend on the incorporated metal ions [10–22]. Metal-substituted POMs possess a higher negative charge density than the saturated parent POMs due to the substitution of a high oxidation state W^{6+} ion by a low oxidation state M^{n+} ion (usually n = 1–3). One of the promising approaches toward the synthesis of this kind of material is combining metal-substituted POMs with organic or metal–organic fragments

to make inorganic–organic hybrid-based LPOMs. Various POM-based inorganic–organic hybrids with interesting structural and functional properties were reported [23–25]. In this field, a certified fact is that the synthesis of such hybrids depends on the selection of POMs as inorganic building blocks and organic ligands as structure-directing and functional components. Therefore, the careful choice of POM species and organic ligands are vital for the synthesis of hybrids with intriguing topologies and improved properties. The utilization of organic fragments as a solvent or coordinated with metal centers in the metal-substituted POM compounds can improve physical and chemical properties of these compounds. Most metal-substituted POM hybrids contain N-donor organic ligands. In these structures, organic fragments not only act as charge-compensation cations, but also as multidentate chelating agents to coordinate TM or Ln cations. This highlights the significant role of organic ligands as stabilizing agents in forming hybrid structures. The general structures discussed in this review are summarized in Figure 1.
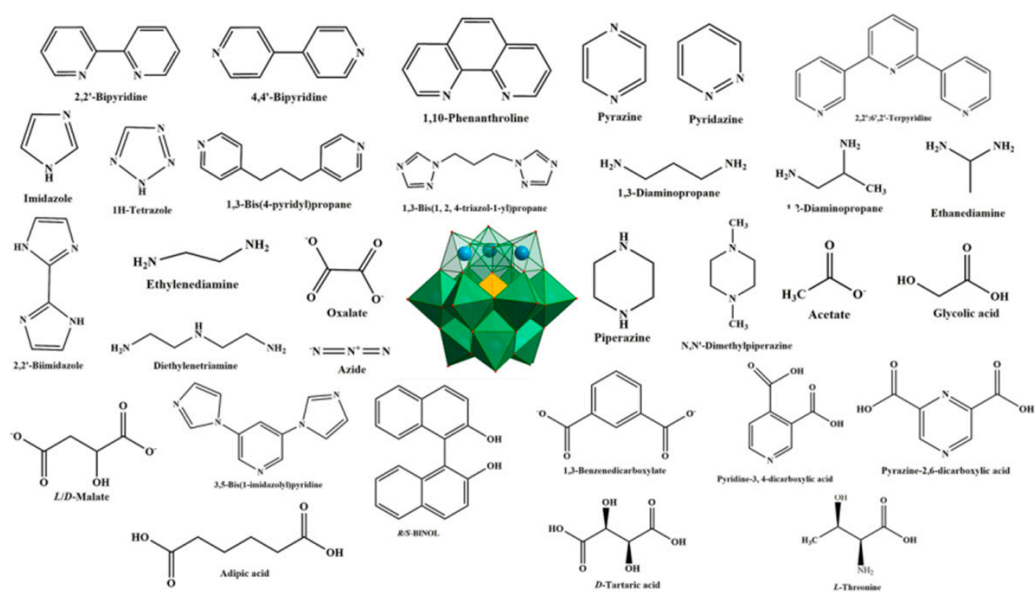

Figure 1. Some organic ligands employed to inorganic–organic hybrids based on lacunary Keggin-type polyoxometalates in the literature.

In the present review, we highlight the most important investigations of inorganic–organic hybrid compounds combining LPOMs with TM and Ln centers. This field of research reveals a great variety of N/O-donor ligands and their potential roles in the assembly of metal-substituted POMs that have not been previously reviewed. Therefore, this review provides a comprehensive description of the different roles of various ligands in their interaction with these relevant inorganic clusters.

2. Inorganic–Organic Hybrids Based on TMSPs

TM-substituted polyoxometalates (TMSPs) are an important class of materials [26,27]. Compared to nonlacunary heteropolyoxometalates, the localized surface charge of LPOMs have made them reactive building blocks for the construction of these hybrids. They are commonly used as excellent precursors, since (i) the LPOMs are easy to obtain from intact materials in high yield, (ii) vacant sites are conducive to encapsulate various transition metals, including mixed-valent metal ions, and (iii) the robustness of POMs makes it possible to predict the frameworks of the ultimate products. Hundreds of different types of LPOMs saturated by TMs or even TM complexes have been reported in recent years [28–31]. However, the introduction of an organic ligand in TMSPs has a pivotal impact on the chemical/physical properties or the structural features of the hybrid via synergetic effects between the properties of the POM and those of the ligand. Therefore, the role of the organic ligands as structure-directing agents is predominant in these inorganic–organic hybrid

constructions, a point that is less considered in the compounds containing polyoxometalate clusters. Because of the nucleophilic interaction between POM anions and TM complexes, popular series of inorganic–organic hybrids based on lacunary POMs are composed of discrete structures that TM complexes substituted in the vacant sites of POMs. Many structures are reported that have these characteristics [32–37]. Abundant sandwich-type TMSPs are reported to have a varied nuclear core. Among them are some TM cores that are coordinated to organic ligands. Furthermore, additional TM complexes can have roles of charge compensation or structure-directing and promote the dimension of these TMSPs. For instance, organic solvents such as DMF and DMSO can be appropriate ligands for coordination to the TMSPs [38–41]. Table 1 provides an exhaustive list of various N-/O-donor ligands that can be connected to LPOMs.

2.1. TMSPs with N-Donor Ligands

Metal complexes of lacuna are popular in studies of POM hybrids. For example, Kato et al. studied the interaction of some TM-substituted α-Keggin polyoxotungstates with cis-platinum(II) moieties containing N-donor ligands [42–44]. Magnetic properties are highly dependent on the nature of the bridging ligands. In the $KRb_5[(PW_{10}O_{37})(Ni(H_2O))_2$ $(\mu\text{-}1,1\text{-}N_3)]\cdot19H_2O$ discrete cluster, N_3^- is connected with two Ni^{II} ions substituted in the vacant sites of the polyanion and the relationship between the structural parameters and the value of the magnetic exchange parameter J for $\mu\text{-}1,1\text{-}N_3$ complexes is considered [45].

Multi-dentate N-donor ligands as structure-stabilizing agents can capture and stabilize the in situ-generated TM oligomers or aggregates to construct novel POMs. en is another bidentate N-donor organic fragment that has largely been employed in the TMSPs. Compounds such as $[Ni_6(\mu_3\text{-}OH)_3(en)_3(H_2O)_6(B\text{-}\alpha\text{-}AsW_9O_{34})]\cdot6H_2O$ and $[Ni_6(\mu_3\text{-}OH)_3$ $(en)_3(H_2O)_6(B\text{-}\alpha\text{-}AsW_9O_{34})]\cdot10H_2O$ are important examples of hexa-Ni-substituted POMs based on single lacunary Keggin fragments because they contain the highest number of transition metal ions in known lacunary Keggin *arsenotungstate* monomers [46,47]. Discrete dimers $(H_2en)_2[Cu^{II}_8(en)_4(H_2O)_2(B\text{-}\alpha\text{-}GeW_9O_{34})_2]\cdot5H_2O$ and $(H_2en)_2[Cu^{II}_8(en)_4(H_2O)_2$ $(B\text{-}\alpha\text{-}SiW_9O_{34})_2]\cdot8H_2O$ are constructed from two trivacant Keggin $[B\text{-}\alpha\text{-}XW_9O_{34}]^{10-}$ ($X=Ge^{IV}/Si^{IV}$) fragments and an octa-Cu cluster [48]. In these structures, hydrogen bonding interactions between the nitrogen atoms of en ligands and surface oxygen atoms of polyoxoanions generate extended supramolecular networks [49]. In the case of $H_{10}K_2Na_2[Zr_4(\mu_3\text{-}O)_2$ $(\mu\text{-}OH)_2(en)_2(B\text{-}\alpha\text{-}GeW_{10}O_{37})_2]\cdot4DMF\cdot22H_2O$ as the first Zr-substituted POM with N–Zr–N bonds; however, a 1D chain structure is formed through the connection of potassium cations and sandwich-type polyoxoanion [50]. Another interesting example is the structure of $[Cu(en)_2(H_2O)]_2\{[Cu(en)_2][\alpha\text{-}PCuW_{11}O_{39}Cl]\}\cdot3H_2O$, which is similar to those of $\{[Cu(en)_2$ $(H_2O)][Cu(en)_2]_2[\alpha\text{-}PCuW_{11}O_{39}Cl]\}\cdot6H_2O$ and $[\{Cu(en)_2\}_3(\alpha\text{-}PCuW_{11}O_{39}Cl)]\cdot6H_2O$ [51]. However, the first is an isolated structure whereas the second and third are 1D linear polymeric chains through $[Cu(en)_2]^{2+}$ bridges via Cu–Cl–Cu–O–W linkages [52]. Belt-like hexa-Cu^{II} cluster-substituted POM, $[Cu_6(en)_2(H_2O)_2(B\text{-}\alpha\text{-}GeW_9O_{34})_2]$, in the presence of two $[Cu(en)_2]^{2+}$ units or $[Cu_4(deta)(H_2O)]^{2+}$ complex bridges form a 1D chain structure, as is found in the other similar hexa-Cu^{II} cluster-substituted POM with $Cu(en)_2$ bridges [53,54]. In these cases, the coordination of en ligands on the hexa-CuII cluster increases the number of the TM cations in the sandwich belt. In fact, each $[Cu_6(en)_2(H_2O)_2$ $(B\text{-}\alpha\text{-}GeW_9O_{34})_2]$ as a complete cluster connects four others via four $[Cu(en)_2]^{2+}$ bridges to form a novel 3D framework, which is rare in sandwich-type POMs [55,56]. Similarly, $[Cu^{II}(H_2O)_2]_2[Cu^{II}_8(en)_4(H_2O)_2(B\text{-}\alpha\text{-}SiW_9O_{34})_2]$ displays 3D (3,6)-connected nets with $(4\cdot6^2)\text{-}(4^2\cdot6^4\cdot8^7\cdot10^2)$ topology, which are built by octa-Cu sandwiched polyoxometalate building blocks through copper cation bridges [48].

$[\{Cu_6(\mu_3\text{-}OH)_3(en)_3(H_2O)_3\}(B\text{-}\alpha\text{-}PW_9O_{34})]\cdot7H_2O$ exhibits an unprecedented 3D framework with hexagonal channels enclosed by three interweaved helical chains in the TMSP chemistry [46]. The steric effect of organic ligands is known to be an important factor in the modification of the structure of coordination compounds, and smaller steric hindrance of the organic ligands favored the POM anions functioning as high-connected

linkages in coordination compounds. Thus, the substitution of dap by en organic ligands in the compounds with the same dimeric Keggin polyoxoanions $[(PW_{11}CuO_{39})_2]^{10-}$ results in different dimensionality. $[Cu(en)_2]^{2+}$ fragments have smaller volume and steric hindrance in comparison with $Cu(dap)_2$ and, hence, have easy access to $[(PW_{11}CuO_{39})_2]^{10-}$ dimers to link with their external active oxygen atoms, forming higher-dimensional and higher-connected POM-based hybrid compounds [52,57].

Sandwich-type structures can encapsulate TM clusters. $\{[Cu(dap)_2(H_2O)]_2[Cu_6(dap)_2 (B-\alpha-SiW_9O_{34})_2]\}\cdot4H_2O$ is an example of a sandwich-type structure with a hexa-nuclear ring [58]. Some discrete dimers are also constructed from two trivacant Keggin $[B-\alpha-XW_9O_{34}]^{10-}$ $(X=Ge^{IV}/Si^{IV})$ fragments and a $\{Cu_8(dap)_4\}$ complex [46,48]. The double-cluster complex of $[\{Ni_7(\mu_3-OH)_3O_2(dap)_3(H_2O)_6\}(B-\alpha-PW_9O_{34})][\{Ni_6(\mu_3-OH)_3(dap)_3(H_2O)_6\}(B-\alpha-PW_9O_{34})]$ $[Ni(dap)_2(H_2O)_2]\cdot4.5H_2O$ is a unique structure containing both hexa- and hepta-Ni^{II}-substituted trivacant Keggin clusters of $\{Ni_6(dap)_3PW_9\}$ and $\{Ni_7(dap)_3PW_9\}$ [46]. Linear organic ligands such as dap can link the sandwich POTs as nodes [59,60]. For example, Chen et al. reported a tetra-nuclear $\{Co^{II}_4(Hdap)_2\}$ substituted sandwich-type Keggin germanotungstate unit with $[Co(dap)_2]^{2+}$ bridges that represented the first 2D organic–inorganic hybrid cobalt-substituted sandwich-type polyoxotungstate [61].

$[Ni_6(\mu_3-OH)_3(H_2O)_2(dien)_3(B-\alpha-PW_9O_{34})]\cdot4H_2O$ is the first extended TMSP with a 1D zigzag chain made of Ni and PW_9O_{34} SBUs via corner-sharing between $\{NiO_6\}$ and $\{WO_6\}$ octahedra via intermolecular interactions. This compound contains the highest number of Ni ions in any known lacunary Keggin polyoxotungstate, as well [62]. In addition to its usual coordination mode, dien can bridge between metal centers, as well. For example, a 2D layer-like structure has been recently reported in which $[Bi_2W_{20}O_{70}]^{14-}$ polyanions are linked by $[Cu_2(dien)_2]^{4+}$ bridges [63].

bpyand phen, as rigid organic ligands, are powerful tools controlling the structure of the final product because they can act as structure-stabilizing agents or structure-directing agents to influence coordination geometries or connecting modes of transition-metals in the vacant sites of POTs in the construction of novel TMSPs. In addition, the N-donor groups may also generate hydrogen bonding interactions and π–π interactions in the formation of target structures, which may affect the properties of complexes [64–69]. A survey of the literature shows that investigations on bpy/phen-containing copper-complex-substituted Keggin POTs have been reported extensively [70,71]; however, organic–inorganic hybrid di-copper-bpy/phen-substituted monovacant Keggin POTs have been explored to a limited extent.

Compound $[Cu^I_3(phen)_3Cl_2][Cu^{II}(phen)_2][Cu^{II}_2(phen)_2(\alpha-PW_{11}O_{39})]$ represents the first discrete di-copper-phen complex-substituted monovacant Keggin polyoxotungstate. It is of note that the π–π interactions between adjacent phen rings may play an important role in the structure stabilization of the title compound [43,68]. In the compound $[Cu^I_3(pz)_2(phen)_3]_2[Cu^I(phen)_2][\{Na(H_2O)_2\}\{(V^{IV}_5Cu^{II}O_6)(As^{III}W_9O_{33})_2\}]\cdot6H_2O$, two $\{AsW_9O_{33}\}$ clusters are connected by the mixed hexa-TM ring unit $\{V^{IV}_5Cu^{II}O_6\}$ to form a sandwich-type dimer, which are further bonded in "ABAB" mode by the $\{Na(H_2O)_2\}$ linker, resulting in pure inorganic chains. The unique "L-shaped" trinuclear complex $\{Cu_3(pz)_2(phen)_3\}$ is supported together via staggered π–π interactions to generate extending waveform 2D supramolecular layers, which are further aggregated with their adjacent analogues by complexes $\{Cu(phen)_2\}$ via H-bonding interactions to yield an unprecedented 3D metal–organic network with 1D cavities. The pure inorganic 1D sandwich chains are implanted in the cavities as guest units via supramolecular interactions to form a POMOF 3D framework [72]. In the skeleton of $[Cu^{II}(bpy)(H_2O)][Cu^{II}_2(bpy)_2(H_2O) (\alpha-HPW_{11}O_{39})]\cdot H_2O$, there are three crystallographically unique Cu^{II} cations. They all adopt the square pyramid geometry with two N atoms from 2,2′-bpy ligands and three O atoms from the $[\alpha-PW_{11}O_{39}]^{7-}$ fragments or water molecules. This complex displays a 1D zigzag infinite chain architecture constructed by alternating di-copper-bpy-substituted $[Cu^{II}_2(bpy)_2(H_2O)(\alpha-HPW_{11}O_{39})]$ polyoxoanions with Cu–O linkers. Notably, this com-

pound is a new di-transition metal-bpy-substituted monovacant Keggin phosphotungstate with a 1D dual-bridging chain structure [68].

The reactivity of other nitrogen heterocyclic ligands such as imi has also been studied. It has been shown that imi ligands connect to metal ions via $M–N_{imi}$ bonds, and no $M–C_{imi}$ bond in POMs has been observed to date [73–77]. In addition, numerous studies have shown that imi could interfere with DNA via weak interactions (hydrogen bonds, $\pi–\pi$ stacking, etc.), and then halt cell growth and division [78,79]. Compound $\{[Ag_7(H_2biim)_5][PW_{11}O_{39}]\}·Cl·H_3O$ displays a 2D network featuring dimerized monolacunary Keggin anions $\{PW_{11}O_{39}\}_2$ which are connected through hexanuclear silver clusters. Interestingly, besides $\{Ag_5\}^{5+}$ clusters, there are other kinds of argentophilic $\{Ag_4\}^{4+}$ clusters coexisting in this compound [80]. Liu et al. reported three hexa-nuclear-substituted sandwich-type arsenotungstates [81]. The transition metal ions (Ni^{II}, Co^{II}, and Mn^{II}) and Na^+ are alternately coordinated in the six-membered central belt by $[\alpha-AsW_9O_{33}]^{9-}$ units, taz, and water molecules. The contribution of nitrogen atoms of the ligands in the formation of hydrogen bonding network leads to the fortification of the structures [81]. Htz as a rigid multifunctional ligand can provide four sequent electron-donating nitrogen atoms to coordinate to metals with the smaller steric hindrance. Many metal–organic frameworks based on Htz ligands exhibit intriguing topologies and interesting magnetic, absorptive, and photophysical properties, having diverse coordination/bridging modes [82,83]. For example, in $\{[Cu_8(tz)_8(Htz)_4(H_2O)_5][PMo^{VI}_{10}Mo^V O_{39}]\}·\sim 10H_2O$, the six-nuclear copper clusters are bridged by the tz ligands to form wave-like layers by the μ_2-Htz ligands. The polyoxomolybdate anions act as the eight-connected node to link the layers into a 3D framework [84].

2.2. TMSPs with O-Donor Ligands

O-donor ligands have been comparatively less studied than flexible nitrogen donating ligands for the design and synthesis of new hybrids. As a peculiar branch of POMs, considerable attention has been directed toward POM-based metal carbonyl derivatives in recent years because of their unique structures and potential catalytic properties [85–88]. For example, $Na_2H_2[(CH_3)_4N]_6[Te_2W_{20}O_{70}\{Re(CO)_3\}_2]·20H_2O$ is a monomeric tellurotungstate(IV)-supported rhenium carbonyl derivative similar to that of the previously reported tricarbonyl metal polyoxoanion complexes $[X_2W_{20}O_{70}\{M(CO)_3\}_2]^{12-}$ (X = Sb, Bi and M = Re, Mn) composed of two identical $\{B-\beta-TeW_9O_{33}\}$ units joined by two $\{WO_6\}$ octahedra. Furthermore, two Re atoms and two central W atoms are located in the same plane and each carbonyl rhenium group fac-$\{Re(CO)_3\}^+$ is in the "out-of-pocket" structural motif [88].

Acetate has been frequently used as a bridging ligand to connect different fragments. For example, in the monomeric structure of $[\gamma-H_2SiW_{10}O_{36}Pd_2(OAc)_2]^{4-}$, Pd atoms are bridged by two bidentate acetate ligands [89]. However, the synthesis is usually performed in acetate buffer solution [90]. Crown-shaped Ru-substituted arsenotungstate $[As_4W_{40}O_{140}\{Ru_2(OAc)\}_2]·22H_2O$ present a new acetate-bridged Ru-substituted arsenotungstate. $[As_4W_{40}O_{140}]^{28-}$ cyclic unit embeds two $[Ru_2(OAc)]^{7+}$ segments in its cavities. A bidentate acetate ligand connects two diametrically opposed Ru atoms in a $(\mu_2-\eta^1:\eta^1)$ fashion. As far as we know, such a crown-shaped acetate-bridged Ru-substituted arsenotungstate is the first report that supports the structural novelty of this rare compound [91]. Kholdeeva, Kortz, and co-workers reported isolated polyanions with unprecedented hexazirconium and hexa-hafnium core and the metal ions occupying the vertices of an octahedron that is accommodated by two (B-α-AsW$_9$O$_{33}$) fragments. The two $\{AsW_9\}$ units are not eclipsed, leaving a cavity perfectly suitable to host the M_6 unit. Furthermore, five bridging acetate ligands lead to stronger bonding between metal centers [92]. The first carboxylic group decorated arsenotungstate was reported in 2015 [93]. Each Mn^{II} ion in the $Na_{15}[(Mn^{II}(COOH))_3(AsW_9O_{33})_2]·15H_2O$ is chelated with four oxygen atoms (μ_3-O) from four $\{WO_6\}$ octahedra belonging to two different $\{AsW_9\}$ units and edge-sharing with two adjacent $\{NaO_6\}$ groups. The most interesting structural feature is that three carboxy groups are separately bonded to three manganese ions.

$[Ni(en)(H_2O)_4]_3[Ni_6(en)_3(Tris)(1,3-bdc)_{1.5}(B-\alpha-PW_9O_{34})]_2\cdot 8H_2O$ represents the first 2D polyoxometalate cluster organic frameworks with honeycomb-like lattice consisting of $[Ni_6(en)_3(Tris)(B-\alpha-PW_9O_{34})]$ structural building units linked by 1,3-bdc ligands. Although the honeycomb-like lattice-based POMs and organic ligands have been investigated, there is no example based on TMSPs as structural building units. It is remarkable that $H[Ni_{0.5}(en)(H_2O)][Ni_6(en)_3(OAc)_2(Tris)(H_2O)_2(B-\alpha-PW_9O_{34})]\cdot 5H_2O$ is functionalized by three types of organic ligands, which is rare in POMs. Furthermore, the nitrogen atoms of the Tris ligand incorporate in hydrogen bonding and help to expand the structure [94]. Subjoining of multi-dentate organic ligands such as tartaric acid and glycolic acid into tetranuclear sandwich-type $[Zr_4(H_2O)_2(\mu_3-O)_2(GeW_{10}O_{37})_2]$ cluster not only helps in the fortification of the sandwich-type cluster, but also, in some cases, induces chirality in the polyoxometalates [95]. Utilization of the dicarboxylato ligands such as $[OOC(CH_2)_4COO]^{2-}$ (adipate), instead of monocarboxylate ligands, can lead to the oligomeric structure. As shown in the dimeric helical $Na_2K_{12}[Ni(H_2O)_6][(SiW_9O_{34})_2(OH)_6Ni_8(C_6H_8O_4)_3]\cdot 40H_2O$ structure, three adipato linkers connect two $\{SiW_9Ni_4\}$ units (Figure 2) [96]. Liu et al. reported unique nona-Mn^{II}-encapsulated sandwich-type species in which the utilization of three oxalate ligands lead to the formation of planar hexagonal $\{Mn_6\}$ core. This structure was further connected to another three external Mn^{II} cations and constructed a 1D oxalate-bridging high-nuclear Mn-sandwiched antimonotungstate chain [97]. The utilization of chiral ligands and transfer of chirality to achiral LPOM units has been reported by using L- or D-tartrate units (tart) in the large polyoxoanion compound $[\alpha-P_2W_{15}O_{56}]^{12}$ [98]. In another interesting study, Ishimoto et al. successfully prepared a BINOL-functionalized lacunary Keggin-type POM for the asymmetric oxidation of thioanisole [99]. This is especially true in POMs, which contain multiple metal centers that are subject to rapid racemization via water exchange, partial hydrolysis, or fluxional rearrangements. As a result, it is often challenging to discriminate between enantiomers and/or diastereomers, and even more formidable to achieve partial or complete resolution. The polytungstate assembly of $[(\alpha-P_2W_{16}O_{59})Zr_2(\mu_3-O)(mal)]_2^{18-}$ consists of two divacant $[\alpha-P_2W_{16}O_{59}]^{12-}$ anions linked by four Zr cations and is constitutionally similar to the centrosymmetric complex, $[Zr_4(\mu_3-O)_2(\mu_2-OH)_2(H_2O)_4(P_2W_{16}O_{59})_2]^{14-}$, reported by Pope et al. [100]. While in it, the μ_2-OH and terminal aqua ligands are replaced by the oxygens of the ligating malates (from carboxylate and hydroxo moieties) [101]. Changing organic units to D/L-mandelic acid has been seen in similar architecture [102]. Wang et al. also reported four similar chiral sandwich-type compounds consisting of tetra-Zr^{IV}-substituted sandwich-type Keggin polyoxoanion and L-/D-mal fragments. The most striking structural feature of $(NH_4)_3Na_2K_5[Zr_4(\mu_3-O)_2(L-mal)(D-mal)(B-\alpha-SiW_{10}O_{37})_2]$ relative to similar compounds is that each $[Zr_4(\mu_3-O)_2(L-mal)(D-mal)(B-\alpha-SiW_{10}O_{37})_2]^{10-}$ polyoxoanion joins adjacent six K^+ bridges and each K^+ bridge links to adjacent three $[Zr_4(\mu_3-O)_2(L-mal)(D-mal)(B-\alpha-SiW_{10}O_{37})_2]^{10-}$ polyoxoanions, leading to a 2D layer. Furthermore, adjacent 2D layers are interconnected by two Na^+ cations, forming a 3D framework [103].
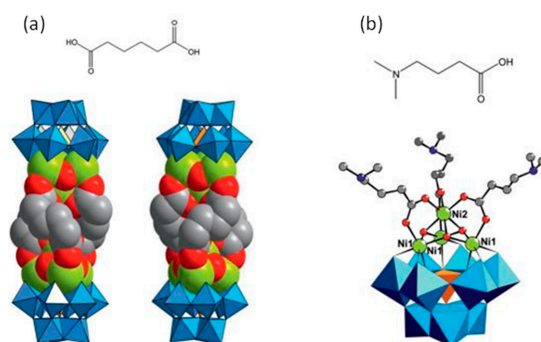
Figure 2. (**a**) Structure of $Na_2K_{12}[Ni(H_2O)_6][(SiW_9O_{34})_2(OH)_6Ni_8(C_6H_8O_4)_3]\cdot 40H_2O$ hybrid with adipic acid as ligand; (**b**) structure of $Na_{1.5}K_{2.5}[Ni(H_2O)_6]_{0.5}(SiW_9O_{34})(OH)_3Ni_4(C_6H_{13}NO_2)_3]\cdot 17H_2O$ hybrid with dimethylaminobutiric acid as ligand [96].

Table 1. Summary of inorganic–organic hybrids based on TMSPs with N-/O-donor ligands.

Compound	LPOM	Metal	Ligand	Ref.
$[(CH_3)_4N]_3[\alpha\text{-}PW_{11}O_{39}\{cis\text{-}Pt(NH_3)_2\}_2]\cdot10H_2O$ $[(CH_3)_4N]_4[\alpha\text{-}SiW_{11}O_{39}\{cis\text{-}Pt(NH_3)_2\}_2]\cdot13H_2O$ $[(CH_3)_4N]_4[\alpha\text{-}GeW_{11}O_{39}\{cis\text{-}Pt(NH_3)_2\}_2]\cdot11H_2O$	mono	Pt	amine	[42]
$[(CH_3)_4N]_4H[\alpha\text{-}AlW_{11}O_{39}\{cis\text{-}Pt(NH_3)_2\}_2]\cdot11H_2O$ $[(CH_3)_4N]_4H[\alpha\text{-}BW_{11}O_{39}\{cis\text{-}Pt(NH_3)_2\}_2]\cdot9H_2O$ $Cs_4[\alpha\text{-}GeW_{11}O_{39}\{Pt(bpy)\}_2]\cdot10H_2O$ $Cs_{3.5}H_{0.5}[\alpha\text{-}GeW_{11}O_{39}\{Pt(phen)\}_2]\cdot3H_2O$	mono	Pt	amine 2,2′-bipyridine 1,10-phenanthroline	[43]
$[(CH_3)_4N]_4H[\alpha\text{-}PW_{11}O_{39}\{cis\text{-}Pt^{II}(Me_2ppz)\}]\cdot5H_2O$	mono	Pt	N,N'-dimethylpiperazine	[44]
$KRb_5[(PW_{10}O_{37})(Ni(H_2O))_2(\mu\text{-}1,1\text{-}N_3)]\cdot19H_2O$	di	Ni	azide	[45]
$[Ni_6(\mu_3\text{-}OH)_3(en)_3(H_2O)_6(B\text{-}\alpha\text{-}AsW_9O_{34})]\cdot6H_2O$ $[\{Ni_7(\mu_3\text{-}OH)_3O_2(dap)_3(H_2O)_6\}(B\text{-}\alpha\text{-}PW_9O_{34})]$ $[\{Ni_6(\mu_3\text{-}OH)_3(dap)_3(H_2O)_6\}$ $(B\text{-}\alpha\text{-}PW_9O_{34})][Ni(dap)_2(H_2O)_2]\cdot4.5H_2O$	tri	Ni	ethylenediamine 1,2-diaminopropane	[46]
$[Ni_6(\mu_3\text{-}OH)_3(en)_3(H_2O)_6(B\text{-}\alpha\text{-}AsW_9O_{34})]\cdot10H_2O$	tri	Ni	ethylenediamine	[47]
$(H_2en)_2[Cu^{II}_8(en)_4(H_2O)_2(B\text{-}\alpha\text{-}GeW_9O_{34})_2]\cdot5H_2O$ $(H_2en)_2[Cu^{II}_8(en)_4(H_2O)_2(B\text{-}\alpha\text{-}SiW_9O_{34})_2]\cdot8H_2O$ $[Cu^{II}(H_2O)_2]_2[Cu^{II}_8(en)_4(H_2O)_2(B\text{-}\alpha\text{-}SiW_9O_{34})_2]$ $[Cu(dap)(H_2O)_3]_2[\{Cu_8(dap)_4(H_2O)_2\}(B\text{-}\alpha\text{-}SiW_9O_{34})_2]\cdot6H_2O$ $[Cu^{II}(H_2O)_2]H_2[Cu^{II}_8(dap)_4(H_2O)_2(B\text{-}\alpha\text{-}GeW_9O_{34})_2]$ $[Cu^{I}(2,2'\text{-}bpy)(4,4'\text{-}bpy)]_2[\{Cu^{I}_2(2,2'\text{-}bpy)_2(4,4'\text{-}bpy)]_2$ $[Cu^{I}_2Cu^{II}_6(2,2'\text{-}bpy)_2(4,4'\text{-}bpy)_2(B\text{-}\alpha\text{-}GeW_9O_{34})_2\}]\cdot2H_2O$	tri	Cu	ethylenediamine 1,2-diaminopropane 2,2′-bipyridine 4,4′-bipyridine	[48]
$[H_2en]_5[(B\text{-}\alpha\text{-}SiW_9O_{34})_2\ Mn^{III}_4Mn^{II}_2O_4(H_2O)_2(Hen)_2]\cdot8H_2O$ $[H_2ppz]_4[H_21,3\text{-}dap]_2[(B\text{-}\alpha\text{-}SiW_9O_{34})_2$ $Mn^{III}_4Mn^{II}_2O_4(H_2O)_2(ppz)_2]\cdot6H_2OH_2[H_2ppz]_4[(B\text{-}\alpha\text{-}SiW_9O_{34})_2$ $Mn^{III}_4Mn^{II}_2O_4(H_2O)_2(Hppz)_2]\cdot8H_2O$	tri	Mn	ethylenediamine piperazine 1,3-diaminopropane	[49]
$H_{10}K_2Na_2[Zr_4(\mu_3\text{-}O)_2(\mu\text{-}OH)_2(en)_2$ $(B\text{-}\alpha\text{-}GeW_{10}O_{37})_2]\cdot4DMF\cdot22H_2O$ $H_{10}K_4[Zr_4(\mu_3\text{-}O)_2(\mu\text{-}OH)_2(dap)_2$ $(B\text{-}\alpha\text{-}GeW_{10}O_{37})_2]\cdot6DMF\cdot18H_2O$	di	Zr	ethylenediamine 1,2-diaminopropane	[50]
$[Cu(en)_2(H_2O)]_2\{[Cu(en)_2][\alpha\text{-}PCuW_{11}O_{39}Cl]\}\cdot3H_2O$ $\{[Cu(en)_2(H_2O)][Cu(en)_2]_2[\alpha\text{-}PCuW_{11}O_{39}Cl]\}\cdot6H_2O$ $[\{Cu(en)_2\}_3(\alpha\text{-}PCuW_{11}O_{39}Cl)]\cdot6H_2O$	mono	Cu	ethylenediamine	[51]
$\{[Cu(en)_2(H_2O)]_2[Cu(en)_2][\alpha\text{-}XCuW_{11}O_{39}]\}\cdot5H_2O$ $(X = Si^{IV}/Ge^{IV})$, $\{[Cu(deta)(H_2O)_2]_2[Cu(deta)(H_2O)][\alpha\text{-}XCuW_{11}O_{39}]\}\cdot5H_2O$ $(X = Ge^{IV}/Si^{IV})$	mono	Cu	ethylenediamine diethylenetriamine	[52]
$[Cu(en)_2(H_2O)]_2[Cu(en)_2][Cu_6(en)_2(H_2O)_2$ $(B\text{-}\alpha\text{-}AsW_9O_{34})_2]\cdot en\cdot9H_2O$ $[Cu(dap)_2]_3[Cu_6(dap)_2(H_2O)_2\ (B\text{-}\alpha\text{-}AsW_9O_{34})_2]\cdot4H_2O$	tri	Cu	ethylenediamine 1,2-diaminopropane	[53]
$[Cu(en)_2]\{[Cu_2(en)_2(\mu\text{-}1,1\text{-}N_3)_2(H_2O)]_2[Cu_6(en)_2(H_2O)_2$ $(B\text{-}\alpha\text{-}PW_9O_{34})_2]\}\cdot6H_2O$	tri	Cu	ethylenediamine	[54]
$[Cu(dap)_2]_2\{[Cu(dap)_2(H_2O)]_2[Cu_6(dap)_2$ $(B\text{-}\alpha\text{-}SiW_9O_{34})_2]\}\cdot4H_2O$	tri	Cu	1,2-diaminopropane	[58]
$[Cu(dien)(H_2O)]_2\{[Cu(dien)(H_2O)]_2[Cu(dien)(H_2O)_2]_2$ $[Cu_4(SiW_9O_{34})_2]\}\cdot5H_2O$ $[Zn(dap)_2(H_2O)]_2\{[Zn(dap)_2]_2[Zn_4(Hdap)_2(PW_9O_{34})_2]\}\cdot8H_2O$ $[Zn(dap)_2(H_2O)]_4[Zn(dap)_2]_2\{(dap)_2\{[Zn(dap)_2]_2[Zn_4(HSiW_9O_{34})_2]\}$ $\{[Zn(dap)_2(H_2O)]_2[Zn_4(HSiW_9O_{34})_2]\}\}\cdot13H_2O$	tri	Cu, Zn	diethylenetriamine 1,2-diaminopropane	[59]
$[Cu(H_2O)_2]H_2[Cu_8(dap)_4(H_2O)_2(\alpha\text{-}B\text{-}GeW_9O_{34})_2]$	tri	Cu	1,2-diaminopropane	[60]
$\{[Co(dap)_2(H_2O)]_2[Co(dap)_2]_2[Co_4(Hdap)_2$ $(B\text{-}\alpha\text{-}HGeW_9O_{34})_2]\}\cdot7H_2O$	tri	Co	1,2-diaminopropane	[61]
$[Ni_6(\mu_3\text{-}OH)_3(H_2O)_2(dien)_3(B\text{-}\alpha\text{-}PW_9O_{34})]\cdot4H_2O$ $[Ni_6(\mu_3\text{-}OH)_3(H_2O)_6(dap)_3(B\text{-}\alpha\text{-}XW_9O_{34})]$ (X = Si, P)	tri	Ni	diethylenetriamine diaminopropane	[62]
$[Cu(dien)(H_2O)]_2[Cu_2(dien)_2]_2H_2[Bi_2W_{20}O_{70}]\cdot15H_2O$	tri	Cu	diethylenetriamine	[63]
$[Cu_2(phen)_2(\mu\text{-}ox)]\{[Cu(phen)(H_2O)_2]$ $[Cu_4(H_2O)_4Cu_2(phen)_2(AsW_9O_{33})_2]\}\cdot6H_2O$	tri	Cu	oxalate 1,10-phenanthroline	[65]
$[Cu(bpy)(H_2O)][H_2PW_{11}O_{39}Cu_2(bpy)_2(H_2O)(OH)]\cdot1.5H_2O$	mono	Cu	2,2′-bipyridine	[66]

Table 1. *Cont.*

Compound	LPOM	Metal	Ligand	Ref.
$[Cu^I_3(phen)_3Cl_2][Cu^{II}(phen)_2][Cu^{II}_2(phen)_2(\alpha\text{-}PW_{11}O_{39})]$ $(Cuphen)_2[Cu(phen)_2]_2[Cu_6phen_2(GeW_9O_{34})_2]\cdot 2H_2O$	tri	Cu	1,10-phenanthroline	[67]
$[\{Cu^I_3(phen)\}_3Cl_2]\{[Cu^{II}(phen)_2][Cu^{II}_2(phen)]\}_2(\alpha\text{-}PW_{11}O_{39})$ $Na[Cu^{II}_2(bpy)_2(OH)_2][Cu^{II}_2(bpy)_2(H_2O)(\alpha\text{-}PW_{11}O_{39})]\cdot 3H_2O$ $[Cu^{II}(bpy)(H_2O)][Cu^{II}_2(bpy)_2(H_2O)(\alpha\text{-}HPW_{11}O_{39})]\cdot H_2O$	mono	Cu	2,2′-bipyridine 1,10-phenanthroline	[68]
$[H_2AsW_{11}O_{39}][Cu_3(bpy)_3(H_2O)_2(OH)]\cdot 2H_2O$	mono	Cu	2,2′-bipyridine	[69]
$[Cu^I(H_2O)(Hbpp)_2]\subset\{[Cu^I(bpp)]_2[PW_{11}Cu^{II}O_{39}]\}$	mono	Cu	1,3-bis(4-pyridyl)propane	[70]
$[\{Si_2W_{22}Cu_2O_{78}(H_2O)\}\{Cu_2(phen)_2(H_2O)(ac)_2\}_2]^{8-}$ $[\{SiW_{11}O_{39}Cu(H_2O)\}\{Cu_2(phen)_2(H_2O)(ac)_2\}]^{4-}$	mono	Cu	acetate 1,10-phenanthroline	[71]
$[Cu_3(pz)_2(phen)_3]_2[Cu^I(phen)_2][\{Na(H_2O)_2\}\{(V^{IV}_5Cu^{II}O_6)(As^{III}W_9O_{33})_2\}]\cdot 6H_2O$	tri	V, Cu	1,10-phenanthroline pyrazine	[72]
$[\{Na(H_2O)_2\}_3\{M(imi)\}_3(SbW_9O_{33})_2]^{9-}$	tri	M = Co, Ni, Zn, Mn	imidazole	[73]
$[\{K(H_2O)_{0.5}\}_2\{K_2(H_2O)_3\}\{Ni(H_2O)(en)_2\}_2\{Ni_4(H_2O)_2(PW_9O_{34})_2\}]$ $[Cu_6(Himi)_6\{As^{III}W_9O_{33}\}_2]\cdot 5H_2O$ $(H_2btp)_4[Fe^{III}_2Fe^{II}_2(H_2O)_2(AsW_9O_{34})_2]\cdot 4H_2O$	tri	Ni, Cu, Fe	ethanediamine imidazole 1,3-bis(1,2,4-triazol-1-yl)propane	[74]
$[Na(H_2O)_2]_3[C_3H_5N_2]_2[SbW_9O_{33}]_2[Fe^{II}(C_3H_4N_2)]_3\cdot 4H_2O$	tri	Fe	imidazole	[75]
$\{Na_{0.7}M_{5.3}(H_2O)_2(imi)_2(Himi)(SbW_9O_{33})_2\}^{6-}$	tri	Ni, Co	imidazole	[76]
$[M_6(imi)_6(B\text{-}\alpha\text{-}AsW_9O_{33})_2]^{6-}$	tri	Mn, Ni, Zn, Cu	imidazole	[77]
$\{[Ag_7(H_2biim)_5][PW_{11}O_{39}]\}\cdot Cl\cdot H_3O$	mono	Ag	2,2′-Biimidazole	[80]
$\{[Cu_8(tz)_8(Htz)_4(H_2O)_5][PMo^{VI}_{10}Mo^VO_{39}]\}\cdot 10H_2O$	mono	Cu	1H-tetrazole	[84]
$K_8[(OC)_3Mn(A\text{-}\alpha\text{-}H_2GeW_9O_{34})]\cdot 10H_2O$ $K_8[(OC)_3Mn(A\text{-}\alpha\text{-}H_2SiW_9O_{34})]\cdot 11H_2O$	tri	Mn	carbonyl	[85]
$(YOH_2)_3(CO_3)(A\text{-}\alpha\text{-}PW_9O_{34})_2{}^{11-}$	tri	Y	carbonate	[86]
$(NH_4)_3H_5[\{Mn_4(H_2O)_{10}\}(\beta\text{-}BiW_9O_{33})_2\{Mn(CO)_3\}_2]\cdot 31H_2O$ $Na_6[(CH_3)_4N]_2[\{Mn_4(H_2O)_{10}\}(\beta\text{-}SbW_9O_{33})_2\{Mn(CO)_3\}_2]\cdot 36H_2O$ $[(CH_3)_4N]_2[Mn(H_2O)_6]_2[\{Mn_{3.5}W_{0.5}(H_2O)_{10}\}(\beta\text{-}SbW_9O_{33})_2\{Mn(CO)_3\}_2]\cdot 12H_2O$ $[(CH_3)_4N]_2[Mn(H_2O)_6]_2[\{Mn_{3.5}W_{0.5}(H_2O)_{10}\}(\beta\text{-}BiW_9O_{33})_2\{Mn(CO)_3\}_2]\cdot 12H_2O$	tri	Mn	carbonyl	[87]
$Na_2H_2[(CH_3)_4N]_6[Te_2W_{20}O_{70}\{Re(CO)_3\}_2]\cdot 20H_2O$	tri	Re	carbonyl	[88]
$[\gamma\text{-}H_2SiW_{10}O_{36}Pd_2(OAc)_2]^{4-}$	di	Pd	acetate	[89]
$K_4H_6[Zr_4(OH)_6(CH_3COO)_2(\alpha\text{-}PW_{10}O_{37})_2]\cdot 23H_2O$	di	Zr	acetate	[90]
$[H_2N(CH_3)_2]_{14}[As_4W_{40}O_{140}\{Ru_2(CH_3COO)\}_2]\cdot 22\,H_2O$	tri	Ru	acetate	[91]
$Cs_6Na_5[Zr_6O_4(OH)_4(H_2O)_2(CH_3COO)_5(AsW_9O_{33})_2]\cdot 80H_2O$ $Cs_6Na_5[Hf_6O_4(OH)_4(H_2O)_2(CH_3COO)_5(AsW_9O_{33})_2]\cdot 80H_2O$	tri	Zr, Hf	acetate	[92]
$Na_{15}[(Mn^{II}(COOH))_3(AsW_9O_{33})_2]\cdot 15H_2O$	tri	Mn	acetate	[93]
$H[Ni_{0.5}(en)(H_2O)][Ni_6(en)_3(OAc)_2(Tris)(H_2O)_2(B\text{-}\alpha\text{-}PW_9O_{34})]\cdot 5H_2O$ $[Ni(en)_2][Ni_6(en)_3(\mu_3\text{-}OH)_3(1,3\text{-}bdc)(H_2O)_2(B\text{-}\alpha\text{-}PW_9O_{34})]\cdot 9H_2O$ $[Ni(en)(H_2O)_4]_3[Ni_6(en)_3(Tris)(1,3\text{-}bdc)_{1.5}(H_2O)_2(B\text{-}\alpha\text{-}PW_9O_{34})]\cdot 8H_2O$	tri	Ni	ethylenediamine acetate tris(hydroxymethyl)aminomethane 1,3-benzenedicarboxylate	[94]
$K_2H_{10}[Zr_4(H_2O)_2(\mu\text{-}OH)(\mu_3\text{-}O)_2(D\text{-}tartH)(GeW_{10}O_{37})_2]\cdot 27H_2O$ $K_2H_{10}[Zr_4(H_2O)_2(\mu_3\text{-}O)_2(gly)_2(GeW_{10}O_{37})_2]\cdot 32H_2O$	di	Zr	D-tartaric acid glycolic acid	[95]
$Na_{1.5}K_{2.5}[Ni(H_2O)_6]_{0.5}[(SiW_9O_{34})(OH)_3Ni_4(C_6H_{13}NO_2)_3]\cdot 17H_2O$ $Na_2K_{12}[Ni(H_2O)_6][(SiW_9O_{34})_2(OH)_6Ni_8(C_6H_8O_4)_3]\cdot 40H_2O$ $Na_6K_8[(SiW_9O_{34})_2(OH)_6Ni_8(C_{10}H_8O_4)_3]\cdot 45H_2O$	tri	Ni	dimethylaminobutyric acid adipic acid p-phenylenediacetic acid	[96]
$Na_2H_4\{[Mn(H_2O)_3]_3[Mn(H_2O)_2]_2[Mn(H_2O)][Mn(C_2O_4)]_3[B\text{-}\alpha\text{-}SbW_9O_{33}]_2\}\cdot 31H_2O$	tri	Mn	oxalic acid	[97]
$TBA_4[\gamma\text{-}SiTi_2W_{10}O_{36}(\mu\text{-}OH)_2(\mu\text{-}BINOLate)]$	di	Ti	(R)/(S)-1,1′-bi-2-naphthol	[99]
$Na_7(NH_4)_5[\{Zr_4(OH)_6(OAc)_2\}(SiW_{10}O_{37})_2]\cdot 20H_2O$	di	Zr	acetate	[102]
$(NH_4)_4(TMA)_4[Zr_4(\mu_3\text{-}O)_2(L\text{-}/D\text{-}mal)_2(B\text{-}\alpha\text{-}HSiW_{10}O_{37})_2]$ $(NH_4)_4(TMA)_4[Zr_4(\mu_3\text{-}O)_2(L\text{-}/D\text{-}mal)_2(B\text{-}\alpha\text{-}PW_{10}O_{37})_2]$	di	Zr	L/D malate	[103]

Table 1. *Cont.*

Compound	LPOM	Metal	Ligand	Ref.
{[Cu$_5$(2,2′-bpy)$_5$(H$_2$O)][GeW$_9$O$_{34}$]}$_2$·7H$_2$O	tri	Cu	2,2′-bipyridine	[104]
Na[{Cu(2,2′-bpy)(imi)}{Cu(2,2′-bpy)}$_2$AsW$_9$O$_{33}$As(OH)]·8H$_2$O	tri	Cu	2,2′-bipyridine imidazole	[105]
Na(H$_2$O)$_6$[Co$_3$(OH)(pydz)$_4$(H$_2$O)$_7$][Co$_6$(PW$_{10}$O$_{37}$)$_2$(pydz)$_4$(H$_2$O)$_6$]·43H$_2$O	di	Co	pyridazine	[106]
H$_8$K$_3$Na$_5$[Zr$_6$(μ$_3$-O)$_3$(OH)$_3$(OAc)(H$_2$O)(β-GeW$_{10}$O$_{37}$)$_3$]·20H$_2$O H$_6$K$_4$Na$_{12}$[{Zr$_5$(μ$_3$-OH)$_4$(OH)$_2$}@{Zr$_2$(OAc)$_2$(α-GeW$_{10}$O$_{38}$)$_2$}$_2$]·22H$_2$O H$_4$Na$_2$[Na$_6$(H$_2$O)$_{22}$][Zr$_4$(μ$_3$-O)$_2$(OH)$_2$(OAc)$_2$(α-GeW$_{10}$O$_{37}$)$_2$]·32H$_2$O	di	Zr	acetate	[107]
(NH$_4$)$_3$Na$_5$K$_6$[Zr$_4$(μ$_3$-O)$_2$(μ-OH)$_2$(ox)$_2$(SiW$_{10}$O$_{37}$)$_2$]·23H$_2$O	di	Zr	oxalate	[108]
Na$_2$H$_4$[Fe$_4$(H$_2$O)$_8$(3, 4-pdc)$_2$(B-β-SbW$_9$O$_{33}$)$_2$]·40H$_2$O	tri	Fe	pyridine-3, 4-dicarboxylic acid	[109]

3. Inorganic–Organic Hybrids Based on RESPs

It is apparent that most mentioned RE-POMs are purely inorganic, and the investigations of organic–inorganic hybrids based on RE-POMs are relatively scarce. Although the simultaneous presence of organic and LPOM ligands that are bound to RE centers is also rare, one can expect that their properties are conveyed to novel hybrid molecules [110]. Occasionally, organic solvents can be connected to metal centers in the POM-based structures. For example, solvents such as acetone, DMSO, and DMF can play the role of a ligand in the dimeric, 1D, and 2D inorganic–organic hybrids based on RESPs by coordinating to metal centers [111,112]. By considering structural features, organic ligands with their functional groups reduce distances between RE centers and facilitate the formation of polynuclear fragments. Thus, in this section, we discuss the role of these interactions in the stability and structural features of rare-earth-substituted inorganic–organic hybrids. The tendency of RE centers to carboxylate groups results in effective interactions between these fragments. Naruke and co-workers reported [Ce$_3$(CO$_3$)(SbW$_9$O$_{33}$)(W$_5$O$_{18}$)$_3$]$^{18-}$ anion with two different types of POMs. In the crystal structure, the triangular [Ce$_3$(CO$_3$)]$^{7+}$ core was surrounded by one trivacant [B-α-SbW$_9$O$_{33}$]$^{9-}$ and three monolacunary Lindqvist anions [W$_5$O$_{18}$]$^{6-}$ [113]. The presence of carbonate in the structure led to the isolation of a compound that was isomorphous to another structure, previously reported by the authors [114].

Acetic acid has been frequently used as a bridging agent in the synthesis of inorganic–organic hybrids because of its small size and tendency to RE metals [115]. In the dimeric structures of {RE(α-XW$_{11}$O$_{39}$)(H$_2$O)}$_2$ [X = Si, Ge, P], acetic acid units act as linkers via (η^2, μ-1,1) fashion, connecting two RE centers. The atomic radius of metals has an important role in the construction of such compounds (Table 2) [116–119]. When Na$_9$[B-α-AsW$_9$O$_{33}$] as precursor reacts to RE ions, it is involved in decomposition and rearrangement reactions that leads to the formation of [B-b-AsW$_9$O$_{33}$]$^{-9}$, {W$_3$O$_{13}$}, {W$_2$O$_{10}$}, and {WO$_6$} fragments. These components are coordinated with RE cations while acetate groups act as ancillary ligands [120].

Amino acids, as a type of carboxyl-and-amino-containing flexible multidentate ligand, are outstanding candidates for performing as organic modifiers in the building of novel structures [121,122]. In this regard, four gly amino acids linked two {RE(α-BW$_{11}$O$_{39}$)} sub-units by sharing O atoms in μ$_2$-O or μ$_3$-O modes. Neighboring [RE$_2$(gly)$_4$(α-BW$_{11}$O$_{39}$)$_2$]$^{12-}$ units were oppositely aligned in a staggered fashion in which N–H···O hydrogen bonds between gly molecule and surface O atoms of POM units as well as Van der Waals interactions generated the 3D supramolecular framework [123]. The polyoxoanion skeletons of three kinds of $_L$-ala-decorated and RE-incorporated arsenotungstate hybrids are similar. It can be designated as two [As$_2$W$_{19}$O$_{68}$]$^{16-}$ polyanions encapsulating an ala-decorated W-O-RE heterometallic cluster ([Eu$_4$W$_5$(H$_2$O)$_{10}$(ala)$_3$O$_{14}$]$^{14+}$, [RE$_4$W$_6$(H$_2$O)$_8$(ala)$_4$O$_{15}$(OH)$_2$]$^{16+}$ (RE = Gd^{III}, Tb^{III}), and [RE$_4$W$_6$(H$_2$O)$_{10}$(ala)$_2$O$_{15}$(OH)$_2$]$^{16+}$ (RE = Dy^{III}, Ho^{III}, Er^{III}, Yb^{III},

Lu^{III}), concluding in a four-leaf-clover-shaped tetrameric structure. However, the major inconsistency in the ala-decorated W-O-RE heterometallic clusters lies in the number of ala molecules, which may result from the different coordination geometries of RE ions and the various construction modes of W-O-RE heterometallic clusters. It should be mentioned that the carboxyl groups of ala ligands only coordinate with the W centers in the compounds containing Dy^{III}, Ho^{III}, Er^{III}, Yb^{III}, and Lu^{III} ions, and they not only link the W centers together but also combine RE ions in the other compounds [124].

Table 2. List of bridging ligands and their characterization in the dimeric inorganic–organic hybrids based on RESPs.

Ligand	RE⋯RE Distance (Å)	RE-O$_{carboxylate}$ (Å)	RE-O$_{POM}$	Compound	Ref
Acetic acid	4.085	2.418, 2.450	2.259–2.290	[{Yb(α-SiW$_{11}$O$_{39}$)(H$_2$O)}$_2$(μ-OAc)$_2$]$^{12-}$	[116]
⌐	4.148	2.460, 2.505	2.319–2.360	[{Eu(α-SiW$_{11}$O$_{39}$)(H$_2$O)}$_2$(μ-OAc)$_2$]$^{12-}$	[117]
⌐	4.133	2.446, 2.492	2.317–2.349	[{Gd(α-SiW$_{11}$O$_{39}$)(H$_2$O)}$_2$(μ-OAc)$_2$]$^{12-}$	[117]
⌐	4.111	2.432, 2.472	2.293–2.349	[{Tb(α-SiW$_{11}$O$_{39}$)(H$_2$O)}$_2$(μ-OAc)$_2$]$^{12-}$	[117]
⌐	4.103	2.436, 2.454	2.290–2.339	[{Dy(α-SiW$_{11}$O$_{39}$)(H$_2$O)}$_2$(μ-OAc)$_2$]$^{12-}$	[117]
⌐	4.086	2.413, 2.458	2.275–2.315	[{Ho(α-SiW$_{11}$O$_{39}$)(H$_2$O)}$_2$(μ-OAc)$_2$]$^{12-}$	[117]
⌐	4.070	2.410, 2.432	2.273–2.320	[{Er(α-SiW$_{11}$O$_{39}$)(H$_2$O)}$_2$(μ-OAc)$_2$]$^{12-}$	[117]
⌐	4.065	2.412, 2.441	2.275–2.291	[{Tm(α-SiW$_{11}$O$_{39}$)(H$_2$O)}$_2$(μ-OAc)$_2$]$^{12-}$	[117]
⌐	4.082	2.419, 2.437	2.291–2.337	[{Y(α-SiW$_{11}$O$_{39}$)(H$_2$O)}$_2$(μ-OAc)$_2$]$^{12-}$	[118]
⌐	4.110	2.430, 2.450	2.300–2.351	[{Y(α- GeW$_{11}$O$_{39}$)(H$_2$O)}$_2$(μ-OAc)$_2$]$^{12-}$	[118]
⌐	4.154	2.502, 2.503, 2.525	2.365–2.404	[{Sm(α-PW$_{11}$O$_{39}$)(H$_2$O)(η^2,μ-1,1)-OAc }$_2$]$^{10-}$	[119]
⌐	4.131	2.474, 2.486, 2.515	2.334–2.362	[{Eu(α-PW$_{11}$O$_{39}$)(H$_2$O)(η^2,μ-1,1)-OAc }$_2$]$^{10-}$	[119]
⌐	4.078	2.424, 2.459, 2.475	2.312–2.369	[{Gd(α-PW$_{11}$O$_{39}$)(H$_2$O)(η^2,μ-1,1)-OAc }$_2$]$^{10-}$	[119]
⌐	4.106	2.446, 2.489, 2.456	2.106–2.359	[{Tb(α-PW$_{11}$O$_{39}$)(H$_2$O)(η^2,μ-1,1)-OAc }$_2$]$^{10-}$	[119]
⌐	4.068	2.437, 2.451, 2.453	2.292–2.341	[{Ho(α-PW$_{11}$O$_{39}$)(H$_2$O)(η^2,μ-1,1)-OAc}$_2$]$^{10-}$	[119]
⌐	4.121	2.462, 2.482, 2.485	2.327–2.384	[{Er(α-PW$_{11}$O$_{39}$)(H$_2$O)(η^2,μ-1,1)- OAc }$_2$]$^{10-}$	[119]
Oxalic acid	6.163	2.363, 2.402	2.252–2.294	{[(α-PW$_{11}$O$_{39}$)Y(H$_2$O)]$_2$(ox)}$^{10-}$	[125]
⌐	6.160	2.362, 2.370	2.251–2.291	{[(α-PW$_{11}$O$_{39}$)Dy(H$_2$O)]$_2$(ox)}$^{10-}$	[125]
⌐	6.136	2.353	2.203–2.286	{[(α-PW$_{11}$O$_{39}$)Ho(H$_2$O)]$_2$(ox)}$^{10-}$	[125]
⌐	6.161	2.373, 2.409	2.247–2.310	{[(α-PW$_{11}$O$_{39}$)Er(H$_2$O)]$_2$(ox)}$^{10-}$	[125]
⌐	6.360	2.295, 2.414	1.983–2.143	{(α-x-PW$_{10}$O$_{38}$)Tm$_2$(ox)(H$_2$O)$_2$}$^{3-}$	[125]

Although ox ligands, such as the aforementioned ligands containing carboxylate groups, act as a linkage in the dimer of {RE(α-XW$_{11}$O$_{39}$)} subunits, their distances between RE centers are different (Table 2) [125]. In some cases, this ligand imposes polynuclear structures and deduces tetrameric moieties [126,127]. Tartaric acid compared to oxalic acid is more flexible, but their carboxylate groups can be completely or partially deprotonated. Hence, two {RE$_2$(AsW$_9$O$_{33}$)} subunits can be linked by two series of non-equivalent tartaric acid segments in an unusual fashion [128]. For the dimeric polyoxotungstate [Ho(tart)(α-PW$_{11}$O$_{39}$)]$_2^{16-}$, the tartrate anion connects two Ho^{III} ions by one carboxyl O atom and one hydroxyl O atom from each end of the tart ligand. Furthermore, two tartrate anions displayed a type of mesomeric configuration with the co-existence of the *D*-tartrate anion and *L*-tartrate anion, which played a significant role in understanding the organic carboxylic acid functionalization. Both two nonequivalent eight-coordinate Ho^{III} centers demonstrated distorted square antiprism configurations, which are all defined by four O donors from the two tartrate fragments and four O atoms from the lacunary site of the [α-PW$_{11}$O$_{39}$]$^{7-}$ polyanion [129]. K$_{11}$LiH$_{21}$[RE$_3$(H$_2$O)$_7${RE$_2$(H$_2$O)$_4$As$_2$W$_{19}$O$_{68}$(WO$_2$)$_2$ (C$_6$O$_7$H$_4$)$_2$}$_3$]·nH$_2$O (RE = Y, Tb, Dy, Ho, Er, Tm, Yb, Lu) is the first high-nuclear RE metal-substitute arsenotungstate aggregate with citric bridges. In these hybrids, the citrate fragments link RE centers and {WO$_2$} units to form trimeric structures [130]. Two Dy ions occupy non-adjacent sites of lacunary {AsW$_{10}$O$_{38}$} polyanion, and each of them is coordinated to a tridentate citric acid ligand. Strong hydrogen bonding resulting from lattice water molecules has fortified the architecture [131]. In the dimeric structure of K$_{20}$Li$_2$[RE$_3$(μ_3-OH)(H$_2$O)$_8$(AsW$_9$O$_{33}$)(AsW$_{10}$O$_{35}$(mal))]$_2$·17H$_2$O (RE = Dy, Tb, Gd, Eu, and Sm) a tri-RE cluster [RE$_3$(μ_3-OH)(H$_2$O)$_8$]$^{8+}$ linked {AsW$_{10}$O$_{35}$(mal)} and {AsW$_9$O$_{33}$} build-

ing blocks by sharing carboxylate groups of mal ligands [132]. Structural characterization of $Na_4H_8[\{Pr(H_2O)_2\}_2\{As_2W_{19}O_{68}\}\{WO_2(mal)\}_2]\cdot24H_2O$ revealed that the Pr^{III} ions formed a 1D infinite helical chain-like architecture by hinging between organo-functionalized $[\{As_2W_{19}O_{68}\}\{WO_2(mal)\}_2]^{18-}$ polyanions. In this case, mal ligands stabilized the structure by the formation of five-membered W–O–C–C–O chelate rings [133].

Bulky ligands containing carboxylate groups may rarely show the bridging effect [134,135]. It was observed that pyridine-4-carboxylic acid can only substitute the water molecules that were coordinated to the bridging lanthanide cation in the structure of $[REK(H_2O)_{12}][RE(H_2O)_6]_2$ $[(H_2O)_4RE(BW_{11}O_{39}H)]_2\cdot20H_2O$ due to the to the steric encumbrance [136]. Ritchie et al. utilized middle RE metals including europium, terbium, and $K_{14}[As_2W_{19}O_{67}(H_2O)]$ units and also Hpic precursors to establish sandwich structures containing two {B-β-AsW$_8$O$_{30}$} subunits. A considerable point was the embedment of three {WO$_2$(pic)} fragments in the $[Tb_2(pic)(H_2O)_2(B\text{-}\beta\text{-}AsW_8O_{30})_2(WO_2(pic))_3]^{10-}$ architecture. The addition of RE components (coordinated to the non-sandwiched {WO$_2$(pic)} unit) led to the development of $[(RE)_8(pic)_6(H_2O)_{22}(B\text{-}\beta\text{-}AsW_8O_{30})_4(WO_2(pic))_6]^{12-}$ (RE = Tb, Eu) structures [137]. In the structure of tetrameric $[RE_2(H_2O)_4(pic)_2W_2O_5][(RE(H_2O)W_2(pic)_2O_4)(B\text{-}\beta\text{-}TeW_8O_{30}H_2)_2]$ (RE = La^{III}, Ce^{III}, Nd^{III}, Sm^{III}, Eu^{III}), Hpic ligand stabilized the structure by connecting W and RE atoms together by forming stable N−O−C−O−W five-membered-rings or N−O−RE−O−W−O six-membered-ring motifs [138]. The reaction of 3,4-pdc, RE ions, and monolacunary silicotungestate polyanions lead to monomeric (3,4-pdc)$_2$RE(H$_2$O)$_2$ SiW$_{11}$O$_{39}$ (RE = La, Pr, Dy) structures. In these structures 3,4-pdc was coordinated to RE centers of RESPs, stabilizing the RE ions on the POM polyanion and preventing them from RE-precipitation. In addition, intermolecular interactions increased the dimensions of architecture [18]. $[PW_{11}O_{39}RE(phen)(H_2O)]_2\cdot(phen)_8\cdot8H_3O$ (RE = Pr, Gd, Sm, La) are the first N-containing organic ligands of functionalized mono-RE-substituted polyoxometalates. These dimeric structures consist of two similar RESPs and coordination of the RE center to the surface oxygen atom of adjacent POM unit adjoins these subunits. Strong π–π interactions between phen moieties coordinated to RE centers form a novel 1D supramolecular chain structure. Other noncovalent interactions such as O−H$\cdots$O, N−H$\cdots$O, and π–π interactions lead to the construction of a 3D supramolecular structure [139].

Organophosphonates as multidentate ligands can provide appropriate electron-donor features and symmetry for the building of high nuclearity RESPs, offering additional stability and opportunity to fine-tune the properties. For example, in the polynuclear clusters of $[Dy_6(ampH)_4(H_2O)_{23}(ampH_2)(PW_{11}O_{39})_2]$ and $[Dy_9(CO_3)_3(ampH)_2(H_2O)_{12}(PW_{10}O_{37})_6]^{35-}$, Dy ions were linked together by bridging oxido ligands from the ampH− ligands to form sandwich-type and propeller-shaped POMs [140].

In some cases, organic ligands not only do not contribute to the increasing nuclearity of a structure but also acts vice versa. A notable example is the work of Li et al. Because of the blocking effect of DMEA, the trimeric polyoxoanion $[Ce_2(H_2O)_6(DMEA)W_4O_9$ $(\alpha\text{-}SeW_9O_{33})_3]$ with an infrequent V-shaped $[Se_3W_{29}O_{103}]^{20-}$ group was obtained (Figure 3a), whereas in the presence of DMAHC, the hexameric polyoxoanion $[Ce_2W_4O_9(H_2O)_7$ $(\alpha\text{-}SeW_9O_{33})_3]_2^{24-}$ was constructed from two equivalent trimeric subunits through two −O−W−O−Ce−O− connections (Figure 3b) [141].
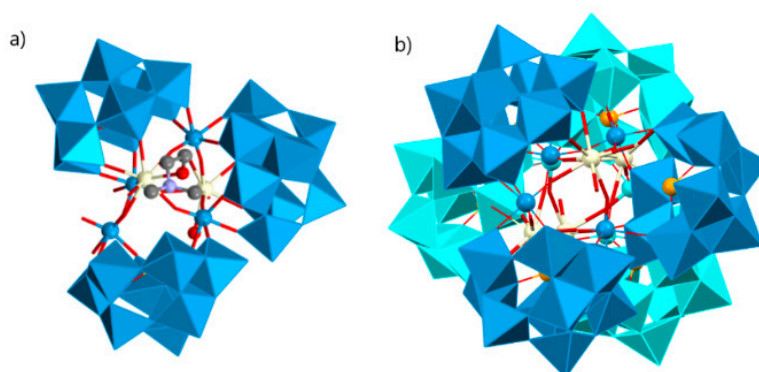
Figure 3. (**a**) Trimeric $[Ce_2(H_2O)_6(DMEA)W_4O_9(\alpha\text{-}SeW_9O_{33})_3]$ cluster. (**b**) Hexameric $[Ce_2W_4O_9(H_2O)_7(\alpha\text{-}SeW_9O_{33})_3]_2$ polyoxoanion structure [141].

4. Inorganic–Organic Hybrids Based on PBTREHDs

In recent years, the design and synthesis of 3d-4f inorganic–organic hybrids based on RESPs has increasingly become an emerging field of research due to an undeniable competitive reaction among strongly oxyphilic RE cations and less active TM cations by highly negative POM precursors in the reaction system. Thus, the discovery and recognition of novel POM-based TM–RE heterometallic derivatives with remarkable structures and properties remains a severe and inquisitorial challenge [142–145]. Such architectures containing TM and RE centers can lead to the formation of discrete to 3D nets. In some cases, N-donor organic fragments are connected to TMs rather than RE metal centers. These TM complexes can be seen as charge-balancing cation, linkage, and directing agents for the construction of high dimension architectures. In the simplest case, complexes of TMs only act as charge-balancing agents for RESPs, such as discrete structures of 1:2 sandwich-type $\{Dy(GeW_{11}O_{39})_2\}$ subunits that are decorated by $[Cu(H_2O)_3]^{2+}$ and $[Cu(H_2en)(Hen)]^{5+}$ coordination cations. These Cu metal centers decrease the negative charge over the heteropolyanions to stabilize the whole framework [146]. In another work, two lacunary $[B\text{-}\alpha\text{-}GeW_9O_{34}]^{10-}$ Keggin moieties were linked together via a rhomb-like $\{Ce^{IV}Cu^{II}_3O_{18}\}$ cluster to form a Weakley-type structure [147]. Compared to the TM-substituted germanotungstate [148], the substitution of one external copper ion by a $\{Ce(OAc)\}^{3+}$ group led to the increase in Cu···Cu distance [147].

Dolbecq, Mialane, and co-workers reported heterometallic cubane clusters of three monolacunary silicotungstates based on $\{LnCu_3(OH)_3O\}$ (Ln = La, Gd, Eu) units [149]. It was observed that the presence of exogenous ligands is essential for obtaining such structures. In addition, the radius of the rare earth center played a crucial role in the dimensionality of the isolated compound [149]. In a similar manner, Wu et al. obtained $\{DyMn_4\}$ cubanes sandwiched by two tetravacant silicotungstates [150]. Other appended cubanes $\{REMn^{III}_4\}$ (RE = Ho^{III}, Tm^{III}, Yb^{III}, Sm^{III}, Gd^{III}, Er^{III}, and Ce^{IV}) were also reported using tetravacant $\{SiW_8O_{31}\}$ ligand [151].

Trilacunary $\{SbW_9O_{33}\}$ can effectively assemble RE ions and TMs into aggregates in the presence of different anions. The resulting compounds $K_5Na_{11}[RE_3(H_2O)_3Ni^{II}_3(H_2O)_6(SbW_9O_{33})_3(WO_4)(CO_3)]\cdot(H_2O)_{40}$ (RE = La^{III}, Pr^{III}, and Nd^{III}) exhibited cyclic trimeric aggregates of three $\{SbW_9O_{33}\}$ units enveloping one CO_3^{2-}-templated and one WO_4^{2-}-templated trigonal-prismatic $\{RE_3(H_2O)_3Ni^{II}_3(H_2O)_6(WO_4)(CO_3)\}$ units [152]. When complexes of TM act as linking centers between RESPs, they can establish high-dimension architectures. The coordination bond interactions and weak interactions between adjacent 1D chains play a significant role in the zigzagging distances and angles of different 1D chains. Numerous structures were reported in which $[Cu(en)_2]^{2+}$ moieties connected to well-known $\{RE(XW_{11}O_{39})_2\}$ (X = P, Si, Ge) dimeric structures. For the dimeric structure of $[RE(PW_{11}O_{39})_2]$ (RE = La, Ce, Pr, Nd, Sm, Er), 1D zigzag chain structures (*via* $Cu(en)_2$ linkage) were extended to 2D sheet structures by weak interactions between the 1D chain and $[Na_2(en)_2(H_2O)_5]^{2+}$ linking cluster presented in other zigzag chain structures. These

resemblance chains were different in bonding distances and angles, due to the coordination bond and weak interactions between adjacent 1D chains [153,154]. {Cu(en)$_2$} unit in the [Cu(en)$_2$]$_4$[RE(PW$_{11}$O$_{39}$)$_2$]$_2^{14-}$ (RE = Ce, Pr) contributed to the generation of 1D zigzag chains which was further extended to 2D supramolecular architectures through hydrogen bonding between nitrogen atoms and [Ce(PW$_{11}$O$_{39}$)$_2$]$^{11-}$ polyanions of the neighboring 1D chain [155]. In the case of H$_8$[Cu(en)$_2$H$_2$O]$_4$[Cu(en)$_2$]{[Cu(en)$_2$][Pr(PW$_{11}$O$_{39}$)$_2$]}$_2$·2en·12H$_2$O, however, weak Cu⋯O electrostatic interactions contributed to making a bidimensional sheet structure [155]. In addition to {Cu(en)$_2$} complexes [156–159], the presentation of other metal centers such as K$^+$ ions were reported to help construct a 1D chain consisting of [RE(XW$_{11}$O$_{39}$)$_2$] building blocks in a series of organic–inorganic hybrids based on lacunary Keggin silico- and germanotungstates [160–164].

Dap, like en segments, is a bidentate ligand that has been used in PBTREHDs crystal structures [165–169]. A behavioral study showed that copper dap complexes generate 1D "dendritic" chain-like TM-Ln heterometallic POMs, whereas en generated a 2D TM-Ln heterometallic sheet architecture [157]. In 2014, a series of 1D antiparallel Cu^{II}-RE^{III} heterometallic germanotungstate polymeric chains were reported in which [Ln(H$_2$O)$_3$ (α-GeW$_{11}$O$_{39}$)]$^{5-}$ moieties were first connected with each other and then these 1D chains were linked together through bridging [Cu(dap)$_2$]$^{2+}$ cations and formed a 1D double-chain architecture [170]. In a similar case, an eight-coordinate RE ion with distorted square antiprism geometry occupy the vacant site of the [α-SiW$_{11}$O$_{39}$]$^{8-}$ polyanion and one free space is coordinated to adjacent polyanions, while two [α-H$_2$SiW$_{11}$O$_{39}$RE(H$_2$O)$_3$] (RE = Ce^{III}, Pr^{III}, Nd^{III}, Sm^{III}, Eu^{III}, Gd^{III}, Tb^{III}, Dy^{III}, Er^{III}) units are connected to adjacent fragments by Cu(dap)$_2$ linkage. There are [Cu(dap)$_2$(H$_2$O)] complexes connected to the surface oxygen of polyanions that, by incorporating hydrogen bonding, established 3D architecture [171].

In a recent study by Wu et al., a rare coordination mode was reported for phen ligands. It was observed that phen ligands preferred Ln over TM. The authors attributed this to the steric hindrance effect in the structure of (Hphen)$_2$[Fe(phen)$_3$]$_2$[Dy(phen)Fe (B-α-GeW$_9$O$_{34}$)]$_2$ [172]. This ligand can generate π–π stacking interactions which help to stabilize the structure [173].

In the 1D chain of [Cu$_2$(tpy)$_2$][RE(H$_2$O)$_3$K(α-HSiW$_{11}$O$_{39}$)]Cl·2H$_2$O (RE = Sm, Eu) compounds, the RE element of {RE-α-SiW$_{11}$} cluster is in connection with {Cu/tpy} segments via Cu–O bonds and they expand a 1D circle-connecting-circle chain [174]. Zhou et al. demonstrated the first example of an organic–inorganic hybrid with a 3D framework based on the RE-containing monovacant silicotungstate Keggin-type POMs and bimpy ligands. [Cu$_{2.5}$(bimpy)$_2$(H$_2$O)$_2$][RE(H$_2$O)$_3$(α-SiW$_{11}$O$_{39}$)]·xH$_2$O [RE = Eu^{III}, Sm^{III}, Ho^{III}, Y^{III}, and Ce^{III}] compounds were isostructural, showing a 3D framework featuring {–SiW$_{11}$–RE–SiW$_{11}$–}$_n$ inorganic chains and {Cu/bimpy} metal–organic ribbons, stemmed from Cu^{2+} ions and bimpy ligands. The adjacent {Cu/bimpy} ribbons were connected by two antiparallel {–SiW$_{11}$–Eu–SiW$_{11}$–}$_n$ chains and created a 2D sheet structure, which was further extended to a 3D framework [175].

The substitution of two water molecules by two thr ligands in the [Fe$_4$(H$_2$O)$_{10}$ (B-β-SbW$_9$O$_{33}$)$_2$]$^{6-}$ polyanion [176] led to the formation of [RE(H$_2$O)$_8$]$_2$[Fe$_4$(H$_2$O)$_8$(thr)$_2$] [B-β-SbW$_9$O$_{33}$]$_2$·22H$_2$O (RE = Pr^{III}, Nd^{III}, Sm^{III}, Eu^{III}, Gd^{III}, Dy^{III}, Lu^{III}) inorganic–organic hybrids in which two nona-coordinated RE centers were attached to terminal oxygen of two {B-β-SbW$_9$O$_{33}$} subunits [177]. Similar architecture was achieved by changing heteropoly to {B-β-AsW$_9$O$_{33}$} subunits [178]. Hpic is another interesting ligand that can generate diverse coordination modes within different coordination geometries of RE ions. The presence of middle RE centers, Gd^{III}, and Dy^{III} ions in the solution containing Hpic, Fe^{III} ion, and {B-α-SbW$_9$} precursor produced discrete structures with different architectures. The molecular structure of these compounds consisted of two types of non-Krebs-type quadripic-inserted [Fe$_2$W$_4$O$_9$(H$_2$O)$_2$(Hpic)$_4$(B-β-SbW$_9$O$_{33}$)$_2$]$^{6-}$ and {[RE(H$_2$O)$_8$]$_2$[Fe$_4$W$_2$O$_7$(H$_2$O)$_4$(pic)$_2$(Hpic)$_2$(B-β-SbW$_9$O$_{33}$)$_2$]}$^{4-}$ moieties. In the first subunit hexa-nuclear {Fe$_2$W$_4$O$_9$(H$_2$O)$_2$(Hpic)$_4$} group and the second subunits, the octa-nuclear

{[Dy(H$_2$O)$_8$]$_2$[Fe$_4$W$_2$O$_7$(H$_2$O)$_4$(pic)$_2$(Hpic)$_2$} group was sandwiched by two {B-β-SbW$_9$O$_{33}$} polyanions. In the case of Ho^{III}, Er^{III} metal ions eight aqua ligands were substituted by four Hpic ligands (Figure 4a). Although both sides of this polyanion were supported by two [RE(H$_2$O)$_5$]^{III} groups, the structure was extended to a 1D heterometallic double chain through the connection of the mentioned atoms in the same direction (Figure 4b). Similar structures were also observed for a series of compounds containing La^{III}, Pr^{III}, Nd^{III}, Sm^{III}, and Eu^{III} cations, in which the connection of one O atom of a carboxylate moiety and one RE^{III} ion of the adjacent unit and the interconnection of these chains constructed a 3D extended framework (Figure 4d) [179].
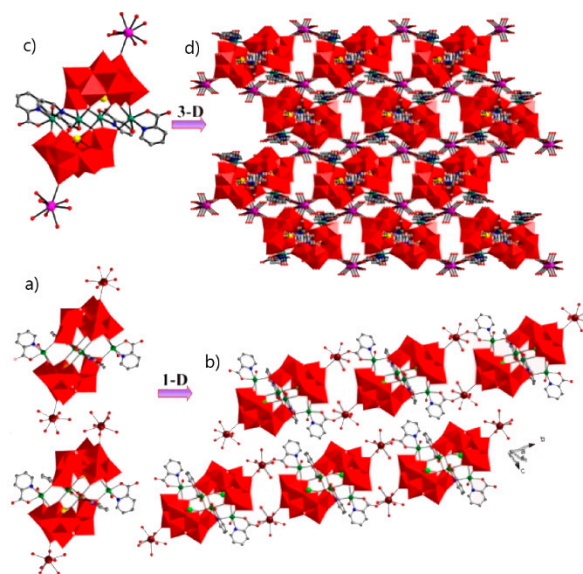

Figure 4. (**a**) View of the pic-substituted Krebs-type unit observed in {[RE(H$_2$O)$_6$]$_2$[Fe$_4$(H$_2$O)$_2$(Hpic)$_2$ (pic)$_2$(B-β-SbW$_9$O$_{33}$)$_2$]}$_2$ (RE = Ho^{III}, Er^{III}). (**b**) One-D double chain observed in previous compounds. (**c**) View of the pic-substituted Krebs-type unit observed in [RE(H$_2$O)$_5$]$_2$[Fe$_4$(H$_2$O)$_2$(pic)$_4$ (B-β-SbW$_9$O$_{33}$)$_2$] [RE = La^{III}, Pr^{III}, Nd^{III}, Sm^{III}, Eu^{III}] compounds. (**d**) Three-D extended framework observed in these structures [179].

Because of high affinity of RE cation linkers to the anionic surface of polyanions, their utilization in synthesis is challenging and almost leads to precipitation [180,181]. By introducing O-donor ligands to the reaction medium Zhao et al. [182] successfully established the 3D K$_4$Na$_4$[Ce$_2$(ox)$_3$(H$_2$O)$_2$]$_2${[Mn(H$_2$O)$_3$]$_2$[Mn$_4$(GeW$_9$O$_{34}$)$_2$(H$_2$O)$_2$]·14H$_2$O hybrid with Weakley sandwich-type structure via tetra Mn^{II} belt and 3d-4f connector. Zhang and co-workers prepared two types of RESP hybrids based on phosphotungstates via oxalate linkages. The {[(α-PW$_{11}$O$_{39}$)RE(H$_2$O)]$_2$(ox)}$^{10-}$ (RE = Y^{III}, Dy^{III}, Ho^{III}, and Er^{III}) hybrid consisted of seven coordinated REs substituted into mono-lacunary phosphotungstates in which one ox ligand interconnected two polyanion units and generated dimeric architectures. In another work, a 3d-4f heterometallic cluster sandwiched phosphotungstate dimers of [Fe$_2$RE(β-PW$_{10}$O$_{37}$)$_2$(tart)]$^{9-}$ (RE = La^{III}, Ce^{IIIIII}, Sm^{III}, Tb^{III}). Fe–O–RE–O–Fe bonds with the support of tart ligands linked [β-PW$_{10}$O$_{37}$]$^{9-}$ polyanions and stabilized the structure [183].

The employment of two types of TMs in the presence of lanthanoid fragments would improve a special property such as the magnetic susceptibility of POM-based clusters. Accordingly, Sato et al. reported five unique sandwich-type polyanions [FeM$_4${RE(L)$_2$}$_2$O$_2$ (A-α-SiW$_9$O$_{34}$)$_2$] (M = Mn^{III}, Cu^{II}; RE = Gd^{III}, Dy^{III}, Lu^{III}; L = acac, hfac) via a three-step successive introduction of metal ions into tri-lacunary Keggin-type POM [A-α-SiW$_9$O$_{34}$]$^{10-}$ in the organic solution. The hepta-nuclear cluster consisted of one central Fe^{II} cation surrounded by four pyramid {MnO$_5$} moieties between two polyoxoanions [184].

5. Inorganic–Organic Hybrids Based on PBTREHD with Mixed Organic Ligands

As mentioned before, O-donor ligands prefer to interact with RE cations in the presence of TM ions; therefore, the introduction of organic fragments containing carboxylate units in the reaction including mono-RE-substituted Keggin polyanions leads to the dinuclear core instead of a cubane moiety [149,185]. Similar dimeric inorganic–organic hybrids based on monolacunary phosphotungstate and germanotungstate polyanions were reported in which a double carboxylate bridging motif coordinated to RE centers that hydrated $\{Cu(en)_2\}$ cations balanced the overall charge of constructions [186–188]. Du's group reported the first 1D ladder-like polyanion chain constructed from monovacant Keggin-type polyanions, RE, TM complexes, and two types of organic ligands. In this case, acetate ions bolt two 2:2-type cerium-substituted $[\alpha\text{-SiW}_{11}O_{39}]^{8-}$ parts. RE ions in these hybrids were coordinated to tetradentate monolacunary polyoxometalate and three carboxylic O atoms from acetate groups and one water molecule via eight-coordinate square antiprism geometry [185]. In the $[Cu(en)_2(H_2O)][Cu(en)_2][Tb(\alpha\text{-PW}_{11}O_{39})(H_2O)_2(ox)Cu(en)]\cdot6H_2O$ hybrid, tetradentate ox ligand acted as a bridge between two terbium associated with $[\alpha\text{-PW}_{11}O_{39}]^{7-}$ anions or two copper ions and constructed a 1D chain along the c-axis and also coordinated to $[Cu(en)_2]$ units [189]. A 1D zigzag chain structure was derived from $[CeGeW_{11}O_{39}]^{5-}$ polyanions by ox and $[Cu(en)_2]^{2+}$ fragments, alternatively. It is interesting that the ox$^-$, as a tetradentate ligand, coordinated to $[Cu(en)_2]^{2+}$ in addition to its linking of two RE centers [186]. In the case of a 2D $\{[Cu(en)_2]_3[Cu(en)(ox)]_2[RE_2(ox)(\alpha\text{-SiW}_{11}O_{39})_2]\}$ (RE = Er^{III}, Sm^{III}) sheet, two $[RE(\alpha\text{-SiW}_{11}O_{39})_2]$ subunits were connected by one free ox moiety and two ox fragments of $\{Cu(en)(ox)\}$ complexes and constructed a dimeric structure (Figure 5b). Two $[Cu(en)(ox)]$ groups linked two $[Cu_2RE_2(ox)(SiW_{11})_2]$ (Figure 5a) as double chain and one $[Cu_3(en)_2]^{2+}$ bridge linked this dimeric structure that was further interconnected to generate a 2D layer [190].
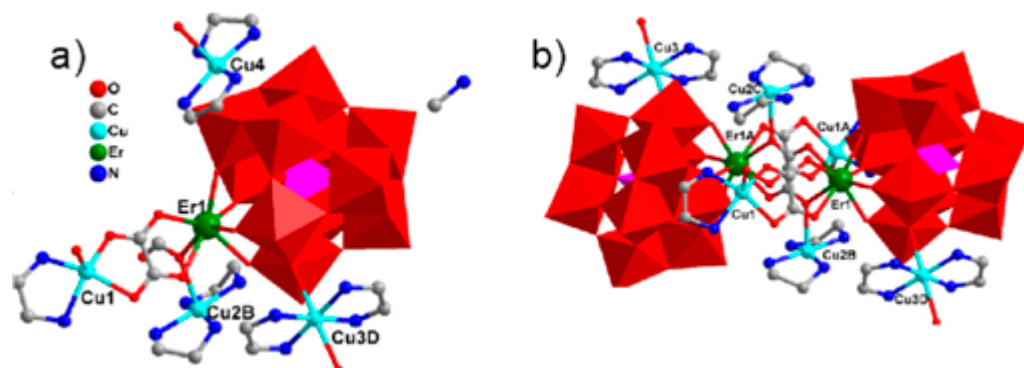
Figure 5. (**a**) Polyhedral and ball-and-stick representation of the asymmetrical unit of $\{[Cu(en)_2]_3[Cu(en)(ox)]_2[RE_2(ox)(\alpha\text{-SiW}_{11}O_{39})_2]\}$. (**b**) The ox-bridging dimeric $\{[Cu(en)_2]_3[Cu(en)(ox)]_2[Er_2(ox)(\alpha\text{-SiW}_{11}O_{39})_2]\}^{6-}$ unit [190].

Zhang et al. separated a family of organic–inorganic hybrids based on silicotungstate derivatives with RE-TM heterometals and 2,6-pzdc and en mixed ligands. 2,6-pzdc and its protonated form have various N/O donor agents that, upon participating in hydrogen bonding, facilitate the construction of supramolecular structures [191]. In $\{[Cu(en)_2]_2[Cu(2,3\text{-pzdc})_2][(\alpha\text{-H}_2SiW_{11}O_{39})Ce(H_2O)]_2\}^{2+}$ hybrids, two carboxylate moieties of two 2,3-pzdc subunits acted as linkage and adjoined cerium centers to construct 1D double-chain architecture. Adjacent N and O atoms of the 2,3-pzdc were linked to Cu^{II} coordinated to the O atom of a polyanion and the last free O atoms of a pentadentate organic ligand trapped by cerium. Ultimately, $[Cu(en)_2]^{2+}$ was linked to the surface of inorganic ligands and thus, hydrogen bonding 3D framework was obtained [192]. Aromatic N-donor organic ligands not only incorporate the coordination sphere of copper ions but also reinforce the fortification of building blocks by weak interactions [193,194]. Cao's group demonstrated that the interaction between the $[RE(PW_{11}O_{39})_2]^{11-}$ (RE = La,

Pr, Eu, Gd, Yb) cluster and dinuclear copper(II)-ox complexes $[Cu_2(bpy)_2(\mu\text{-ox})]^{2+}$ leads to a 1D infinite chain that further extends to 3D nets via π–π interactions of bipyridine rings of adjacent chains [195]. Niu et al. reported organic–inorganic hybrids composed of sandwich-type $[RE(\alpha\text{-PW}_{11}O_{39})_2]^{11-}$ building blocks and a copper complex with two different types of N-donor organic ligands as linkage. When $[RE(\alpha\text{-PW}_{11}O_{39})_2]$ (RE = Ce^{III}, Pr^{III}) dimers were connected by $[Cu(en)(2,2'\text{-bipy})]^{2+}$ and $[Cu(en)_2]^{2+}$, a 1D zigzag chain was formed whilst strong hydrogen bonding constructed a 2D lattice [196]. Another interesting example was observed in a series of some isostructural $[Cu(cyclam)]_2[\{Cu(cyclam)\}_4\{(\alpha\text{-GeW}_{11}O_{39})RE(H_2O)(OAc)\}_2]\cdot18H_2O$ (RE = La−Lu) hybrids where acetate ions connected two $\{(\alpha\text{-GeW}_{11}O_{39})RE\}$ polyanions, while three type $\{Cu(cyclam)\}^{2+}$ moieties had different structural roles: surface-appended antenna unit, linking moieties, and charge-balancing cation [197].

The first inorganic–organic hybrid of RE-substituted tellurotungstates containing three different organic ligands dimethylamine hydrochloride, acetic acid, and IN was reported by Han's group. Accordingly, a family of unique tellurotungstate-based organotin-RE heterometallic hybrids $[H_2N(CH_3)_2]_6H_{12}Na_2\{[Sn(CH_3)W_2O_4(IN)][(B\text{-}\alpha\text{-TeW}_8O_{31})RE(H_2O)(OAc)]_2\}_2\cdot25H_2O$ [RE = Ce^{III}, Pr^{III}, Nd^{III}, Sm^{III}, Eu^{III}, Gd^{III}, Tb^{III}] were synthesized. In these structures, two dimeric $\{[Sn(CH_3)W_2O_4(IN)][(B\text{-}\alpha\text{-TeW}_8O_{31})Nd(H_2O)(OAc)]\}^{10-}$ units were linked by two OAc$^-$ connectors. Two rare tetravacant $[B\text{-}\alpha\text{-TeW}_8O_{31}]^{10-}$ subunits sandwiched a cap-sharing IN-decorated $[W_2O_4(IN)]^{3+}$ fragment. One $[Sn(CH_3)]^{3+}$ group via penta-coordinate square pyramid configuration connected to O atoms of the equatorial belt W centers and eventually, two crystallographically independent RE ions occupied vacant sites of the tetralacunary $[B\text{-}\alpha\text{-TeW}_8O_{31}]^{10-}$ subunits via nonacoordinate severely distorted tricapped trigonal prism geometry to construct the new territory of an inorganic–organic hybrid (Figure 6) [198].
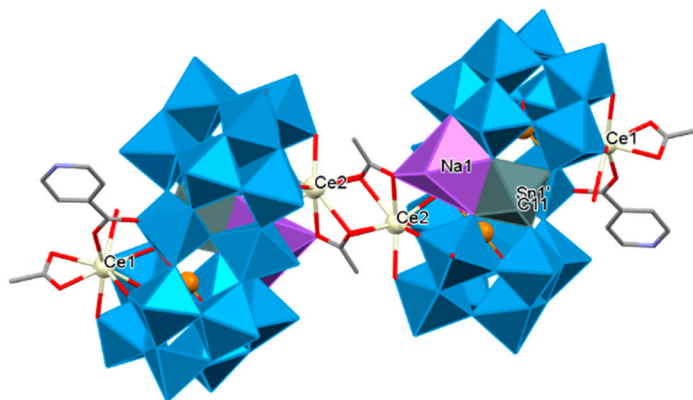
Figure 6. The dimeric skeleton of $Na_2\{[Sn(CH_3)W_2O_4(IN)][(B\text{-}\alpha\text{-TeW}_8O_{31})Ce(H_2O)(OAc)]_2\}_2$ [198].

$[H_2N(CH_3)_2]_8K_2Na_4[RE_2(OAc)_2(H_2O)_4Fe_2(2,5\text{-pdc})_2(B\text{-}\beta\text{-TeW}_9O_{33})_2][RE_2(H_2O)_8Fe_2(2,5\text{-pdc})_2(B\text{-}\beta\text{-TeW}_9O_{33})_2]\cdot50H_2O$ [RE = Eu^{III}, Tb^{III}, Dy^{III}, Er^{III}; 2,5-pdc = 2,5-pyridinedicarboxylic acid] isostructural compounds, owing to the unusual decoration of heterometallic centers by various organic components in the field of POM-based TM−RE heterometallic derivatives, have fascinating structures. On the other hand, two asymmetric sandwich-type subunits, $[RE_2(OAc)_2(H_2O)_4Fe_2(2,5\text{-pdc})_2(B\text{-}\beta\text{-TeW}_9O_{33})_2]^{8-}$ and $[RE_2(H_2O)_8Fe_2(2,5\text{-pdc})_2(B\text{-}\beta\text{-TeW}_9O_{33})_2]^{6-}$, can be regarded as classic Krebs-type $[Fe_4(H_2O)_{10}(\beta\text{-TeW}_9O_{33})_2]^{4-}$ fragments in which two external Fe^{III} ions are substituted by two RE complexes. Among the two O-donor ligands in the structure, only 2,5-pdc as a linkage, incorporating N and O atoms, conduce tetrameric and then 1D chain arrangement [199].

6. Conclusions

The localized surface charge and diverse structures of LPOMs have made them reactive building blocks for the construction of inorganic-organic architectures. The structures

of the lacuna itself as well as the main coordination modes of organic fragments are key parameters that need to be considered. The topology of the final hybrid depends on the number of vacancies generated in the parent structure. Organic fragments, on the other hand, can work as ornaments, bridges, and stabilizers in the whole structure. Since oxo groups in POM surfaces can only bond with limited species of transition metals, the utilization of organic ligands is crucial. In the present work, we highlighted the most important reports of inorganic–organic hybrid structures combining LPOMs with TM and Ln ions and compared the different roles of various ligands in their interaction with relevant Keggin-type POMs. Our results demonstrate a great variety of organic ligands and their important roles in the architecture of metal-substituted POMs.

Author Contributions: Conceptualization, M.M.; writing—original draft preparation, R.K., V.J., F.T., J.T.M.; writing—review and editing, V.J., M.M. All authors have read and agreed to the published version of the manuscript.

Institutional Review Board Statement: Not applicable.

Informed Consent Statement: Not applicable.

Data Availability Statement: Data is contained within the article.

Conflicts of Interest: The authors declare no conflict of interest.

Abbreviations

OAc: ac	Acetate
acac	Acetylacetonate
ala	Alanine
ampH2	(Aminomethyl)phosphonic acid
bdc	Benzenedicarboxylate
bdyl	2,2′-Bipyridinyl
bimpy	3,5-Bis(1-imidazolyl)pyridine
BINOL	(R)- or (S)-1,1′-bi-2-naphthol bipy, bpy: 2,2′-Bipyridine
bpp	1,3-bis(4-pyridyl)propane
btp	1,3-bis(1, 2, 4-triazol-1-yl) propane
cyclam	1,4,8,11-Tetraazacyclotetradecane
dap	Diaminopropane
dien, deta	Diethylenetriamine
DMAHC	dimethylamine hydrochloride
DMEA	N,N-dimethylethanolamine
DMF	Dimethylformamide
DMSO	Dimethyl sulfoxide
en	Ethylenediamine
gly	Glycine
H2biim	2,2′-Biimidazole
hfac	Hexafluoroacetylacetonate
Hpic	2-picolinic acid
Htz	1H-tetrazole
imi	Imidazole
IN	Isonicotinate
Ln	Lanthanoide
LPOM	Lacunary POM

mal	Malate
Me₂ppz	*N,N′*-dimethylpiperazine
ox	Oxalate
PBTREHD	POM-based TM-RE heterometallic derivative
pdc	Pyridine dicarboxylate
phen	1,10-Phenanthroline
pic	Picolinate
POM	Polyoxometalate
POMOF	Polyoxometalate open framewok/Polyoxometalate-based metal–organic framework
POT	Polyoxotungstate
ppz	piperazine
pydz	Pyridazine
pz	Pyrazine
pzdc	Pyrazinedicarboxylic acid
RE	Rare earth
RESP	Rare earth-substituted POM
tart	Tartrate
taz	1,2,4-1H-triazole
TBA	Tetrabutylammonium
thr	Threonine
TM	Transition metal
TMA	Tetramethylammonium
TMSP	Transition metal-substituted POM
tpy	2,2′:6′,2″-terpyridine
Tris	Tris(hydroxymethyl)aminomethane

References

1. Patel, A.; Narkhede, N.; Singh, S.; Pathan, S. Keggin-type lacunary and transition metal substituted polyoxometalates as heterogeneous catalysts: A recent progress. *Catal. Rev.* **2016**, *58*, 337–370. [CrossRef]
2. Ueda, T. Electrochemistry of polyoxometalates: From fundamental aspects to applications. *ChemElectroChem* **2018**, *5*, 823–838. [CrossRef]
3. Lotfian, N.; Heravi, M.M.; Mirzaei, M.; Heidari, B. Applications of inorganic-organic hybrid architectures based on polyoxometalates in catalyzed and photocatalyzed chemical transformations. *Appl. Organomet. Chem.* **2019**, *33*, e4808. [CrossRef]
4. Samaniyan, M.; Mirzaei, M.; Khajavian, R.; Eshtiagh-Hosseini, H.; Streb, C. Heterogeneous catalysis by polyoxometalates in metal–organic frameworks. *ACS Catal.* **2019**, *9*, 10174–10191. [CrossRef]
5. Clemente-Juan, J.M.; Coronado, E.; Gaita-Ariño, A. Magnetic polyoxometalates: From molecular magnetism to molecular spintronics and quantum computing. *Chem. Soc. Rev.* **2012**, *41*, 7464–7478. [CrossRef] [PubMed]
6. Čolović, M.B.; Lacković, M.; Lalatović, J.; Mougharbel, A.S.; Kortz, U.; Krstić, D.Z. Polyoxometalates in Biomedicine: Update and Overview. *Curr. Med. Chem.* **2020**, *27*, 362–379. [CrossRef]
7. Rong, C.; Pope, M.T. Lacunary polyoxometalate anions are. pi.-acceptor ligands. Characterization of some tungstoruthenate (II, III, IV, V) heteropolyanions and their atom-transfer reactivity. *J. Am. Chem. Soc.* **1992**, *114*, 2932–2938. [CrossRef]
8. Anyushin, A.V.; Kondinski, A.; Parac-Vogt, T.N. Hybrid polyoxometalates as post-functionalization platforms: From fundamentals to emerging applications. *Chem. Soc. Rev.* **2020**, *49*, 382–432. [CrossRef]
9. Klemperer, W.G. Introduction to Early Transition Metal Polyoxoanions. In *Inorganic Syntheses*; Ginsberg, A.P., Ed.; John Wiley & Sons, Inc.: Hoboken, NJ, USA, 1990; Volume 27, pp. 71–85.
10. Li, C.; Jimbo, A.; Yamaguchi, K.; Suzuki, K. A protecting group strategy to access stable lacunary polyoxomolybdates for introducing multinuclear metal clusters. *Chem. Sci.* **2021**, *12*, 1240–1244. [CrossRef]
11. Fan, Y.-H.; Li, M.-M.; Dang, D.-B.; Bai, Y.; Li, X.-Z.; Zhao, Y.-P.; Niu, J.-Y. Synthesis, structure and magnetic properties of a two-dimensional polymer based on sandwich-type tetra-cobalt(II)-substituted polyoxotungstate anions and 1-D potassium-chains. *J. Coord. Chem.* **2013**, *66*, 946–957. [CrossRef]
12. Li, M.-X.; Jin, S.-L.; Liu, H.-Z.; Xie, G.-Y.; Chen, M.-Q.; Xu, Z.; You, X.-Z. A novel hydroxo-bridged ferric bisubstituted Keggin heteropolytungstate dimer: Synthesis and crystal structure of (Me₄N)₁₀[Fe₄(OH)₄(PW₁₀O₃₇)₂]·15H₂O. *Polyhedron* **1998**, *17*, 3721–3725. [CrossRef]
13. Chen, W.-C.; Jiao, C.-Q.; Wang, X.-L.; Shao, K.-Z.; Su, Z.-M. Self-assembly of nanoscale lanthanoid-containing selenotungstates: Synthesis, structures, and magnetic studies. *Inorg. Chem.* **2019**, *58*, 12895–12904. [CrossRef]
14. Li, W.-W.; Cai, S.-N.; Tian, Z.-F.; Fan, Y.-H.; Xu, Z.-P.; Bai, Y.; Dang, D.-B. A sandwich-type tungstoantimonate derivative: Synthesis, characterization and catalytic in H₂O₂-based oxidation of cyclooctene. *Inorg. Chem. Commun.* **2019**, *104*, 36–39. [CrossRef]

15. Zhang, G.-H.; Yang, W.-B.; Wu, W.-M.; Wu, X.-Y.; Zhang, L.; Kuang, X.-F.; Wang, S.-S.; Lu, C.-Z. A sandwich-type polyoxometalate for efficient noble-metal-free hydrogen evolution upon visible light irradiation. *J. Catal.* **2019**, *369*, 54–59. [CrossRef]

16. Zhang, Y.; Li, Y.; Pang, J.; Liu, Y.; Li, P.; Chen, L.; Zhao, J. Two penta-RE^{III} encapsulated tetravacant dawson selenotungstates and nanoscale derivatives and their luminescence properties. *Inorg. Chem.* **2019**, *58*, 7078–7090. [CrossRef] [PubMed]

17. Wang, J.; Hao, Q. Thin films of silica particles covered with lanthanide substituted Keggin polyoxometalates and their optical properties. *J. Alloys Compd.* **2009**, *482*, 235–239. [CrossRef]

18. Fashapoyeh, M.A.; Mirzaei, M.; Eshtiagh-Hosseini, H.; Rajagopal, A.; Lechner, M.; Liu, R.; Streb, C. Photochemical and electrochemical hydrogen evolution reactivity of lanthanide-functionalized polyoxotungstates. *Chem. Commun.* **2018**, *54*, 10427–10430. [CrossRef]

19. Cai, J.; Ye, R.; Jia, K.; Qiao, X.; Zhao, L.; Liu, J.; Sun, W. pH-controlled construction of lanthanide clusters from lacunary polyoxometalate with single-molecule magnet behavior. *Inorg. Chem. Commun.* **2020**, *112*, 107694. [CrossRef]

20. Zhang, J.; Qin, C.; Wang, E.; Su, Z.; Xu, L. A novel large heteropolytungstate constructed from two types of lacunary Keggin anions: K$_7$Na$_{13}$[(PW$_{11}$O$_{39}$)$_2$(PW$_9$O$_{34}$)$_2$(W$_2$O$_3$)$_2$]·25H$_2$O. *Inorg. Chim. Acta* **2007**, *360*, 3376–3379. [CrossRef]

21. Li, C.; Mizuno, N.; Yamaguchi, K.; Suzuki, K. Self-Assembly of Anionic Polyoxometalate–Organic Architectures Based on Lacunary Phosphomolybdates and Pyridyl Ligands. *J. Am. Chem. Soc.* **2019**, *141*, 7687–7692. [CrossRef]

22. Aoki, S.; Kurashina, T.; Kasahara, Y.; Nishijima, T.; Nomiya, K. Polyoxometalate (POM)-based, multi-functional, inorganic–organic, hybrid compounds: Syntheses and molecular structures of silanol-and/or siloxane bond-containing species grafted on mono-and tri-lacunary Keggin POMs. *Dalton Trans.* **2011**, *40*, 1243–1253. [CrossRef]

23. Mirzaei, M.; Eshtiagh-Hosseini, H.; Alipour, M.; Frontera, A. Recent developments in the crystal engineering of diverse coordination modes (0–12) for Keggin-type polyoxometalates in hybrid inorganic–organic architectures. *Coord. Chem. Rev.* **2014**, *275*, 1–18. [CrossRef]

24. Taghipour, F.; Mirzaei, M. A survey of interactions in crystal structures of pyrazine-based compounds. *Acta Crystallogr. Sect. C Struct. Chem.* **2019**, *75*, 231–247. [CrossRef] [PubMed]

25. Taleghani, S.; Mirzaei, M.; Eshtiagh-Hosseini, H.; Frontera, A. Tuning the topology of hybrid inorganic–organic materials based on the study of flexible ligands and negative charge of polyoxometalates: A crystal engineering perspective. *Coord. Chem. Rev.* **2016**, *309*, 84–106. [CrossRef]

26. Ma, X.; Li, H.; Chen, L.; Zhao, J. The main progress over the past decade and future outlook on high-nuclear transition-metal substituted polyoxotungstates: From synthetic strategies, structural features to functional properties. *Dalton Trans.* **2016**, *45*, 4935–4960. [CrossRef]

27. Oms, O.; Dolbecq, A.; Mialane, P. Diversity in structures and properties of 3d-incorporating polyoxotungstates. *Chem. Soc. Rev.* **2012**, *41*, 7497–7536. [CrossRef]

28. Guo, L.-Y.; Jagodič, M.; Zeng, S.-Y.; Wang, Z.; Shi, Z.-Q.; Wang, X.-P.; Tung, C.-H.; Sun, D. pH-Controlled assembly of two novel Dawson-sandwiched clusters involving the in situ reorganization of trivacant α-[P$_2$W$_{15}$O$_{56}$]$^{12−}$ into divacant α-[P$_2$W$_{16}$O$_{57}$]$^{8−}$. *Dalton Trans.* **2016**, *45*, 8404–8411. [CrossRef]

29. Cheng, M.; Zhang, Z.; Li, H.-L.; Yang, G.-Y. A new inorganic-organic hybrid transition-metal-substituted polyoxometalate. *Inorg. Chem. Commun.* **2018**, *96*, 69–72. [CrossRef]

30. Mukhacheva, A.A.; Volchek, V.V.; Abramov, P.A.; Sokolov, M.N. Blocking {RhCl}$^{2+}$ disorder in the crystal structure of a [SiW$_{11}$O$_{39}${RhCl}]$^{6−}$ salt: Direct localization of the heterometal in a monosubstituted Keggin anion. *Inorg. Chem. Commun.* **2018**, *89*, 10–12. [CrossRef]

31. Xu, H.; Liu, X.-M.; Su, T.; Chen, W.-C.; Su, Z.-M. Two Ni/Co-substituted sandwich-type germanomolybdates based on an unprecedented trivacant polyanion [α-GeMo$_{10}$O$_{36}$]$^{8−}$. *Dalton Trans.* **2020**, *49*, 977–982. [CrossRef] [PubMed]

32. Bi, L.-H.; Al-Kadamany, G.; Chubarova, E.V.; Dickman, M.H.; Chen, L.; Gopala, D.S.; Richards, R.M.; Keita, B.; Nadjo, L.; Jaensch, H. Organo-ruthenium supported heteropolytungstates: Synthesis, structure, electrochemistry, and oxidation catalysis. *Inorg. Chem.* **2009**, *48*, 10068–10077. [CrossRef]

33. Bi, L.-H.; Kortz, U.; Dickman, M.H.; Keita, B.; Nadjo, L. Trilacunary Heteropolytungstates Functionalized by Organometallic Ruthenium(II),[(RuC$_6$H$_6$)$_2$XW$_9$O$_{34}$]$^{6−}$ (X= Si, Ge). *Inorg. Chem.* **2005**, *44*, 7485–7493. [CrossRef] [PubMed]

34. Bi, L.-H.; Chubarova, E.V.; Nsouli, N.H.; Dickman, M.H.; Kortz, U.; Keita, B.; Nadjo, L. Dilacunary decatungstates functionalized by organometallic ruthenium(II),[{Ru(C$_6$H$_6$)(H$_2$O)}{Ru(C$_6$H$_6$)}(γ-XW$_{10}$O$_{36}$)]$^{4−}$ (X = Si, Ge). *Inorg. Chem.* **2006**, *45*, 8575–8583. [CrossRef] [PubMed]

35. Meng, R.-Q.; Suo, L.; Hou, G.-F.; Liang, J.; Bi, L.-H.; Li, H.-L.; Wu, L.-X. Organo-Ru supported sandwich-type tungstoarsenates: Synthesis, structure and catalytic properties. *CrystEngComm* **2013**, *15*, 5867–5876. [CrossRef]

36. Liu, C.-G.; Liu, S.; Zheng, T. Computational Study of Metal–Dinitrogen Keggin-Type Polyoxometalate Complexes [PW$_{11}$O$_{39}$M^{II}N$_2$]$^{5−}$ (M = Ru, Os, Re, Ir): Bonding Nature and Dinitrogen Splitting. *Inorg. Chem.* **2015**, *54*, 7929–7935. [CrossRef] [PubMed]

37. Sokolov, M.N.; Adonin, S.A.; Mainichev, D.A.; Sinkevich, P.L.; Vicent, C.; Kompankov, N.B.; Gushchin, A.L.; Nadolinny, V.A.; Fedin, V.P. New {RuNO} Polyoxometalate [PW$_{11}$O$_{39}$Ru^{II}(NO)]$^{4−}$: Synthesis and Reactivity. *Inorg. Chem.* **2013**, *52*, 9675–9682. [CrossRef]

38. Sadakane, M.; Tsukuma, D.; Dickman, M.H.; Bassil, B.; Kortz, U.; Higashijima, M.; Ueda, W. Structural characterization of mono-ruthenium substituted Keggin-type silicotungstates. *Dalton Trans.* **2006**, *35*, 4271–4276. [CrossRef]

39. Kikukawa, Y.; Suzuki, K.; Yamaguchi, K.; Mizuno, N. Synthesis, Structure Characterization, and Reversible Transformation of a Cobalt Salt of a Dilacunary γ-Keggin Silicotungstate and Sandwich-Type Di-and Tetracobalt-Containing Silicotungstate Dimers. *Inorg. Chem.* **2013**, *52*, 8644–8652. [CrossRef]

40. Ogo, S.; Shimizu, N.; Nishiki, K.; Yasuda, N.; Mizuta, T.; Sano, T.; Sadakane, M. Preparation and Redox Studies of α_1-and α_2-Isomers of Mono-Ru-Substituted Dawson-type Phosphotungstates with a DMSO Ligand:$[\alpha_1/\alpha_2$-$P_2W_{17}O_{61}Ru^{II}$ (DMSO)$]^{8-}$. *Inorg. Chem.* **2014**, *53*, 3526–3539. [CrossRef]

41. Kikukawa, Y.; Kuroda, Y.; Yamaguchi, K.; Mizuno, N. Diamond-Shaped $[Ag_4]^{4+}$ Cluster Encapsulated by Silicotungstate Ligands: Synthesis and Catalysis of Hydrolytic Oxidation of Silanes. *Angew. Chem. Int. Ed.* **2012**, *51*, 2434–2437. [CrossRef]

42. Kato, C.N.; Suzuki, S.; Ihara, Y.; Aono, K.; Yamashita, R.; Kikuchi, K.; Okamoto, T.; Uno, H. Hydrogen evolution from water under visible-light irradiation using Keggin-type platinum(II)-coordinated phospho-, silico-, and germanotungstates as co-catalysts. *Mod. Res. Catal.* **2016**, *5*, 103–129. [CrossRef]

43. Kato, C.N.; Suzuki, S.; Mizuno, T.; Ihara, Y.; Kurihara, A.; Nagatani, S. Syntheses and characterization of α-Keggin-and α_2-Dawson-type diplatinum(II)-coordinated polyoxotungstates: Effects of skeletal structure, internal element, and nitrogen-containing ligand coordinated to the platinum center for hydrogen production from water under light irradiation. *Catal. Today* **2019**, *332*, 2–10.

44. Kato, C.N.; Nagatani, S.; Mizuno, T. Synthesis, Characterization, and Stability of α-Keggin-Type Polyoxotungstate-Coordinated Mono-Platinum(II) Complex. *Eur. J. Inorg. Chem.* **2019**, *2019*, 517–522. [CrossRef]

45. Mialane, P.; Dolbecq, A.; Riviere, E.; Marrot, J.; Secheresse, F. A Polyoxometalate Containing the $\{Ni_2N_3\}$ Fragment: Ferromagnetic Coupling in a NiII μ-1, 1 Azido Complex with a Large Bridging Angle. *Angew. Chem. Int. Ed.* **2004**, *43*, 2274–2277. [CrossRef] [PubMed]

46. Zhao, J.W.; Jia, H.P.; Zhang, J.; Zheng, S.T.; Yang, G.Y. A Combination of Lacunary Polyoxometalates and High-Nuclear Transition-Metal Clusters under Hydrothermal Conditions. Part II: From Double Cluster, Dimer, and Tetramer to Three-Dimensional Frameworks. *Chem.—Eur. J.* **2007**, *13*, 10030–10045. [CrossRef] [PubMed]

47. Cai, B.; Zhao, J.-W.; Yang, B.-F.; He, H.; Yang, G.-Y. Two Hexa-Ni-Substituted $AsW_9 O_{34}$ Clusters Functionalized by Organic Ligands. *J. Clust. Sci.* **2014**, *25*, 1047–1059. [CrossRef]

48. Zhao, J.W.; Wang, C.M.; Zhang, J.; Zheng, S.T.; Yang, G.Y. Combination of Lacunary Polyoxometalates and High-Nuclear Transition Metal Clusters under Hydrothermal Conditions: IX. A Series of Novel Polyoxotungstates Sandwiched by Octa-Copper Clusters. *Chem.—Eur. J.* **2008**, *14*, 9223–9239. [CrossRef]

49. Xue, H.; Zhao, J.W.; Pan, R.; Yang, B.F.; Yang, G.Y.; Liu, H.S. Diverse Ligand-Functionalized Mixed-Valent Hexamanganese Sandwiched Silicotungstates with Single-Molecule Magnet Behavior. *Chem.—Eur. J.* **2016**, *22*, 12322–12331. [CrossRef]

50. Ni, Z.-H.; Zhang, Z.; Yang, G.-Y. Two New Tetra-Zr(IV)-Substituted Sandwich-Type Polyoxometalates Functionalized by Different Organic Amine Ligands. *J. Clust. Sci.* **2018**, *29*, 1185–1191. [CrossRef]

51. Lisnard, L.; Dolbecq, A.; Mialane, P.; Marrot, J.; Sécheresse, F. Hydrothermal syntheses and characterizations of 0D to 3D polyoxotungstates linked by copper ions. *Inorg. Chim. Acta* **2004**, *357*, 845–852. [CrossRef]

52. Zhao, J.-W.; Zheng, S.-T.; Yang, G.-Y. 0-D and 1-D inorganic–organic composite polyoxotungstates constructed from in-situ generated monocopper^{II}-substituted Keggin polyoxoanions and copperII–organoamine complexes. *J. Solid State Chem.* **2008**, *181*, 2205–2216. [CrossRef]

53. Zhao, J.; Shi, D.; Chen, L.; Cai, X.; Wang, Z.; Ma, P.; Wang, J.; Niu, J. Two organic–inorganic hybrid 1-D and 3-D polyoxotungstates constructed from hexa-Cu^{II} substituted sandwich-type arsenotungstate units. *CrystEngComm* **2012**, *14*, 2797–2806. [CrossRef]

54. Li, Y.-Y.; Zhao, J.-W.; Wei, Q.; Yang, B.-F.; Yang, G.-Y. Synthesis and characterization of a 1D chain-like Cu_6 substituted sandwich-type phosphotungstate with pendant dinuclear Cu–azido complexes. *J. Solid State Chem.* **2014**, *210*, 166–170. [CrossRef]

55. Zhang, Z.; Sun, K.N.; Yang, G.-Y. Two Series of Cu^{II}-Substituted Sandwich-Type Polyoxotungstates Constructed from Trivacant Germanotungstate Fragments. *ChemistrySelect* **2019**, *4*, 7559–7565. [CrossRef]

56. Zhao, J.-W.; Zheng, S.-T.; Li, Z.-H.; Yang, G.-Y. Combination of lacunary polyoxometalates and high-nuclear transition-metal clusters under hydrothermal conditions: First $6^5 \cdot 8$ $CdSO_4$-type 3-D framework built by hexa-Cu^{II} sandwiched polyoxotungstates. *Dalton Trans.* **2009**, 1300–1306. [CrossRef]

57. Li, S.; Zhu, W.; Ma, H.; Pang, H.; Liu, H.; Yu, T. Structure and bifunctional electrocatalytic activity of a novel 3D framework based on dimeric monocopper-substituted polyoxoanions as ten-connected linkages. *RSC Adv.* **2013**, *3*, 9770–9777. [CrossRef]

58. Zheng, S.-T.; Yuan, D.-Q.; Zhang, J.; Yang, G.-Y. Combination of Lacunary Polyoxometalates and High-Nuclear Transition Metal Clusters under Hydrothermal Conditions. 3. Structure and Characterization of $[Cu(enMe)_2]_2\{[Cu(enMe)_2(H_2O)]_2 [Cu_6(enMe)_2 (B-\alpha-SiW_9O_{34})_2]\}\cdot 4H_2O$. *Inorg. Chem.* **2007**, *46*, 4569–4574. [CrossRef]

59. Zheng, S.-T.; Wang, M.H.; Yang, G.-Y. Extended Architectures Constructed from Sandwich Tetra-Metal-Substituted Polyoxotungstates and Transition-Metal Complexes. *Chem.–Asian J.* **2007**, *2*, 1380–1387. [CrossRef]

60. Zhao, J.-W.; Zhang, J.; Zheng, S.-T.; Yang, G.-Y. Combination between lacunary polyoxometalates and high-nuclear transition metal clusters under hydrothermal conditions: First (3,6)-connected framework constructed from sandwich-type polyoxometalate building blocks containing a novel $\{Cu_8\}$ cluster. *Chem. Commun.* **2008**, *5*, 570–572. [CrossRef]

61. Chen, L.; Shi, D.; Zhao, J.; Wang, Y.; Ma, P.; Niu, J. Synthesis, structure and magnetism of a 2-D organic–inorganic hybrid tetra-Co^{II}-substituted sandwich-type Keggin germanotungstate:$\{[Co(dap)_2(H_2O)]_2 [Co(dap)_2]_2[Co_4(Hdap)_2(B-\alpha-HGeW_9O_{34})_2]\}\cdot 7H_2O$. *Inorg. Chem. Commun.* **2011**, *14*, 1052–1056. [CrossRef]

62. Zheng, S.-T.; Yuan, D.-Q.; Jia, H.-P.; Zhang, J.; Yang, G.-Y. Combination between lacunary polyoxometalates and high-nuclear transition metal clusters under hydrothermal conditions: I. from isolated cluster to 1-D chain. *Chem. Commun.* **2007**, *18*, 1858–1860. [CrossRef]

63. Li, J.; Wan, R.; Li, H.; Liu, Y.; Zhang, S.; Ma, P. A new 2-D layer-like organic-inorganic hybrid tungstobismuthate constructed from $[Bi_2W_{20}O_{70}]^{14-}$ units and dimeric $[Cu_2(dien)_2]^{24+}$ complex cations. *J. Mol. Struct.* **2019**, *1181*, 142–147. [CrossRef]

64. Yang, H.; Cao, M.; Gao, S.; Cao, R. A new hybrid constructed from Dawson-like polyoxometalates and dicopper coordination compounds containing a discrete tridecameric water cluster. *J. Mol. Struct.* **2014**, *1056*, 141–145. [CrossRef]

65. Han, Q.; Ma, P.; Zhao, J.; Wang, J.; Niu, J. A novel 1D tungstoarsenate with mixed organic ligands assembled by hexa-Cu sandwiched Keggin units and dinuclear copper-oxalate complexes. *Inorg. Chem. Commun.* **2011**, *14*, 767–770. [CrossRef]

66. Li, B.; Zhao, J.-W.; Zheng, S.-T.; Yang, G.-Y. Hydrothermal synthesis and structure of di-copper^{II}-complex substituted monovacant polyoxotungstate with a 1D chain structure. *Inorg. Chem. Commun.* **2008**, *11*, 1288–1291. [CrossRef]

67. Wang, J.; Du, J.; Niu, J. Novel hexanuclear copper(II)-substituted dimeric tungstogermanates. *CrystEngComm* **2008**, *10*, 972–974. [CrossRef]

68. Zhao, H.-Y.; Dong, D.-P.; Yu, N.-S.; Liu, B.-K.; Lin, X.; Wang, L. Three new organic–inorganic hybrid di-copper-complex substituted monovacant phosphotungstates: Hydrothermal syntheses, structures and properties. *Inorg. Chem. Commun.* **2018**, *88*, 25–29. [CrossRef]

69. Zhao, Z.; Zhou, B.; Su, Z.; Ma, H. Hydrothermal synthesis, structure and properties of copper–bipyridine complexes substituted mono-vacant Keggin arsenotungstate. *Solid State Sci.* **2010**, *12*, 803–807. [CrossRef]

70. Pang, H.; Ma, H.; Yu, Y.; Yang, M.; Xun, Y.; Liu, B. An unusual mono-substituted Keggin anion-chain based 3D framework with 24-membered macrocycles as linker units. *J. Solid State Chem.* **2012**, *186*, 23–28. [CrossRef]

71. Reinoso, S.; Vitoria, P.; Felices, L.S.; Lezama, L.; Gutiérrez-Zorrilla, J.M. Analysis of weak interactions in the crystal packing of inorganic metalorganic hybrids based on Keggin polyoxometalates and dinuclear copper(II)-acetate complexes. *Inorg. Chem.* **2006**, *45*, 108–118. [CrossRef]

72. Wang, K.-P.; Yu, K.; Lv, J.-H.; Zhang, M.-L.; Meng, F.-X.; Zhou, B. A Host–Guest Supercapacitor Electrode Material Based on a Mixed Hexa-Transition Metal Sandwiched Arsenotungstate Chain and Three-Dimensional Supramolecular Metal–Organic Networks with One-Dimensional Cavities. *Inorg. Chem.* **2019**, *58*, 7947–7957. [CrossRef] [PubMed]

73. Cui, R.R.; Wang, H.L.; Yang, X.Y.; Ren, S.H.; Hu, H.M.; Fu, F.; Wang, J.W.; Xue, G.L. Imidazole Coordinated Sandwich-type Antimony Poly-oxotungstates $Na_9[\{Na(H_2O)_2\}_3\{M(C_3H_4N_2)\}_3(SbW_9O_{33})_2]\cdot xH_2O$ (M = Ni^{II}, Co^{II}, Zn^{II}, Mn^{II}). *Chin. J. Chem.* **2007**, *25*, 176–181. [CrossRef]

74. Ma, X.; Yu, K.; Yuan, J.; Cui, L.; Lv, J.; Dai, W.; Zhou, B. Multinuclear transition metal sandwich-type polytungstate derivatives for enhanced electrochemical energy storage and bifunctional electrocatalysis performances. *Inorg. Chem.* **2020**, *59*, 5149–5160. [CrossRef] [PubMed]

75. Sun, M.; Wang, T.; Li, F.; Sun, Z.; Xu, L. A novel sandwich-tungstoantimonate cluster with Fe^{II} ions: Synthesis, magnetic property and electrochemical sensing of dopamine. *New J. Chem.* **2018**, *42*, 7480–7484. [CrossRef]

76. Zhao, H.; Tao, L.; Zhang, F.; Zhang, Y.; Liu, Y.; Xu, H.; Diao, G.; Ni, L. Transition metal substituted sandwich-type polyoxometalates with a strong metal–C(imidazole) bond as anticancer agents. *Chem. Commun.* **2019**, *55*, 1096–1099. [CrossRef] [PubMed]

77. Zhao, Z.; Zhou, B.; Zheng, S.; Su, Z.; Wang, C. Hydrothermal synthesis, crystal structure and magnetic characterization of three hexa-M substituted tungstoarsenates (M = Ni, Zn and Mn). *Inorg. Chim. Acta* **2009**, *362*, 5038–5042. [CrossRef]

78. Shalini, K.; Sharma, P.K.; Kumar, N. Imidazole and its biological activities: A review. *Der Chem. Sin.* **2010**, *1*, 36–47.

79. Zhang, L.; Peng, X.M.; Damu, G.L.; Geng, R.X.; Zhou, C.H. Comprehensive review in current developments of imidazole-based medicinal chemistry. *Med. Res. Rev.* **2014**, *34*, 340–437. [CrossRef]

80. Shi, Z.-Y.; Peng, J.; Li, Y.-G.; Zhang, Z.-Y.; Yu, X.; Alimaje, K.; Wang, X. Assembly of multinuclear Ag complexes and Keggin polyoxometalates adjusted by organic ligands: Syntheses, structures and luminescence. *CrystEngComm* **2013**, *15*, 7583–7588. [CrossRef]

81. Liu, J.-M.; Wang, L.; Yu, K.; Su, Z.-M.; Wang, C.-M.; Wang, C.-M.; Zhou, B.-B. Synthesis, crystal structure and properties of sandwich type compounds based on {AsW$_9$} and a hexa-nuclear unit with three supporting TM-triazole complexes. *New J. Chem.* **2015**, *39*, 1139–1147. [CrossRef]

82. Wu, C.-D.; Lu, C.-Z.; Zhuang, H.-H.; Huang, J.-S. Hydrothermal assembly of a novel three-dimensional framework formed by $[GdMo_{12}O_{42}]^{9-}$ anions and nine coordinated Gd^{III} cations. *J. Am. Chem. Soc.* **2002**, *124*, 3836–3837. [CrossRef]

83. Chen, W.; Li, Y.; Wang, Y.; Wang, E.; Zhang, Z. A new polyoxometalate-based 3d–4f heterometallic aggregate: A model for the design and synthesis of new heterometallic clusters. *Dalton Trans.* **2008**, *7*, 865–867. [CrossRef] [PubMed]

84. Wu, X.-Y.; Yang, W.-B.; Wu, W.-M.; Liao, J.-Z.; Wang, S.-S.; Lu, C.-Z. A inorganic-organic hybrid material constructed from the monolacunary polyoxomolybdates and multi-nuclear copper clusters. *Inorg. Chem. Commun.* **2017**, *76*, 118–121. [CrossRef]

85. Zhao, J.; Wang, J.; Zhao, J.; Ma, P.; Wang, J.; Niu, J. Two novel trivacant Keggin-type polytungstates supported manganese carbonyl derivatives synthesized by degradation of metastable $[\gamma-XW_{10}O_{36}]^{8-}$ (X= Ge^{IV}, Si^{IV}). *Dalton Trans.* **2012**, *41*, 5832–5837. [CrossRef] [PubMed]

86. Fang, X.; Anderson, T.M.; Neiwert, W.A.; Hill, C.L. Yttrium polyoxometalates. Synthesis and characterization of a carbonate-encapsulated sandwich-type complex. *Inorg. Chem.* **2003**, *42*, 8600–8602. [CrossRef]

87. Jia, J.; Zhang, Y.; Zhang, P.; Ma, P.; Zhang, D.; Wang, J.; Niu, J. Synthesis and characterization of a series of novel polyoxometalate-supported carbonyl manganese derivatives. *RSC Adv.* **2016**, *6*, 108335–108342. [CrossRef]

88. Lu, J.; Ma, X.; Wang, P.; Feng, J.; Ma, P.; Niu, J.; Wang, J. Synthesis, characterization and catalytic epoxidation properties of a new tellurotungstate(IV)-supported rhenium carbonyl derivative. *Dalton Trans.* **2019**, *48*, 628–634. [CrossRef] [PubMed]

89. Hirano, T.; Uehara, K.; Kamata, K.; Mizuno, N. Palladium(II) containing γ-Keggin silicodecatungstate that efficiently catalyzes hydration of nitriles. *J. Am. Chem. Soc.* **2012**, *134*, 6425–6433. [CrossRef] [PubMed]

90. Zhang, W.; Liu, S.X.; Zhang, C.D.; Tan, R.K.; Ma, F.J.; Li, S.J.; Zhang, Y.Y. An Acetate-Functionalized Tetranuclear Zirconium Sandwiching Polyoxometalate Complex. *Eur. J. Inorg. Chem.* **2010**, *2010*, 3473–3477. [CrossRef]

91. Han, M.; Niu, Y.; Wan, R.; Xu, Q.; Lu, J.; Ma, P.; Zhang, C.; Niu, J.; Wang, J. A Crown-Shaped Ru-Substituted Arsenotungstate for Selective Oxidation of Sulfides with Hydrogen Peroxide. *Chem.-Eur. J.* **2018**, *24*, 11059–11066. [CrossRef]

92. Al-Kadamany, G.; Mal, S.S.; Milev, B.; Donoeva, B.G.; Maksimovskaya, R.I.; Kholdeeva, O.A.; Kortz, U. Hexazirconium-and Hexahafnium-Containing Tungstoarsenates(III) and Their Oxidation Catalysis Properties. *Chem.-Eur. J.* **2010**, *16*, 11797–11800. [CrossRef] [PubMed]

93. Wu, Q.; Ju, H.; Tao, J.; Chen, Z.; Li, J.; Wang, F.; Cai, Q.; Sun, L.; Pan, X. New Member of Organic Ligand Functionalized TMSP: Synthesis, Characterized and Properties of $Na_{15}[(Mn^{II}(COOH))_3(AsW_9O_{33})_2]\cdot15H_2O$. *J. Clust. Sci.* **2015**, *26*, 1811–1820. [CrossRef]

94. Zhang, Z.; Wang, Y.-L.; Li, H.-L.; Sun, K.-N.; Yang, G.-Y. Syntheses, structures and properties of three organic–inorganic hybrid polyoxotungstates constructed from $\{Ni_6PW_9\}$ building blocks: From isolated clusters to 2-D layers. *CrystEngComm* **2019**, *21*, 2641–2647. [CrossRef]

95. Ni, Z.-H.; Li, H.-L.; Li, X.-Y.; Yang, G.-Y. Zr 4-Substituted polyoxometalate dimers decorated by d-tartaric acid/glycolic acid: Syntheses, structures and optical/electrochemical properties. *CrystEngComm* **2019**, *21*, 876–883. [CrossRef]

96. Rousseau, G.; Rivière, E.; Dolbecq, A.; Marrot, J.; Oms, O.; Mialane, P. Monomeric, Dimeric Helical, and 1D Nickel Polyoxotungstates Structured by Carboxylate Derivatives. *Eur. J. Inorg. Chem.* **2013**, *2013*, 1793–1798. [CrossRef]

97. Liu, J.; Luo, J.; Han, Q.; Cao, J.; Chen, L.; Song, Y.; Zhao, J. Coexistence of long-range ferromagnetic ordering and spin-glass behavior observed in the first inorganic–organic hybrid 1-D oxalate-bridging nona-Mn^{II} sandwiched tungstoantimonate chain. *J. Mater. Chem. C* **2017**, *5*, 2043–2055. [CrossRef]

98. Fang, X.; Anderson, T.M.; Hill, C.L. Enantiomerically Pure Polytungstates: Chirality Transfer through Zirconium Coordination Centers to Nanosized Inorganic Clusters. *Angew. Chem. Int. Ed.* **2005**, *44*, 3540–3544. [CrossRef]

99. Ishimoto, R.; Kamata, K.; Suzuki, K.; Yamaguchi, K.; Mizuno, N. Synthesis and structural characterization of BINOL-modified chiral polyoxometalates. *Dalton Trans.* **2015**, *44*, 10947–10951. [CrossRef]

100. Gaunt, A.J.; May, I.; Collison, D.; Holman, K.T.; Pope, M.T. Polyoxometal cations within polyoxometalate anions. Seven-coordinate uranium and zirconium heteroatom groups in $[(UO_2)_{12}(\mu_3$-$O)_4(\mu_2$-$H_2O)_{12}(P_2W_{15}O_{56})_4]^{32-}$ and $[Zr_4(\mu_3$-$O)_2(\mu_2$-$OH)_2(H_2O)_4(P_2W_{16}O_{59})\ 2]^{14-}$. *J. Mol. Struct.* **2003**, *656*, 101–106. [CrossRef]

101. Fang, X.; Anderson, T.M.; Hou, Y.; Hill, C.L. Stereoisomerism in polyoxometalates: Structural and spectroscopic studies of bis (malate)-functionalized cluster systems. *Chem. Commun.* **2005**, *28*, 5044–5046. [CrossRef]

102. Li, D.; Han, H.; Wang, Y.; Wang, X.; Li, Y.; Wang, E. Modification of tetranuclear zirconium-substituted polyoxometalates–syntheses, structures, and peroxidase-like catalytic activities. *Eur. J. Inorg. Chem.* **2013**, *2013*, 1926–1934. [CrossRef]

103. Wang, Y.-L.; Zhao, J.-W.; Zhang, Z.; Sun, J.-J.; Li, X.-Y.; Yang, B.-F.; Yang, G.-Y. Enantiomeric Polyoxometalates Based on Malate Chirality-Inducing Tetra-ZrIV–Substituted Keggin Dimeric Clusters. *Inorg. Chem.* **2019**, *58*, 4657–4664. [CrossRef]

104. Wang, C.-M.; Zheng, S.-T.; Yang, G.-Y. Novel copper-complex-substituted tungstogermanates. *Inorg. Chem.* **2007**, *46*, 616–618. [CrossRef]

105. Zhao, Z.; Zhou, B.; Su, Z.; Zhu, C. Hydrothermal synthesis, structure and properties of a new arsenotungstate. *J. Solid State Chem.* **2010**, *183*, 332–337. [CrossRef]

106. Guo, L.-Y.; Zeng, S.-Y.; Jagličcić, Z.; Hu, Q.-D.; Wang, S.-X.; Wang, Z.; Sun, D. A pyridazine-bridged sandwiched cluster incorporating planar hexanuclear cobalt ring and bivacant phosphotungstate. *Inorg. Chem.* **2016**, *55*, 9006–9011. [CrossRef]

107. Zhang, Z.; Li, H.-L.; Wang, Y.-L.; Yang, G.-Y. Syntheses, structures, and electrochemical properties of three new acetate-functionalized zirconium-substituted germanotungstates: From dimer to tetramer. *Inorg. Chem.* **2019**, *58*, 2372–2378. [CrossRef]

108. Wang, Y.L.; Zhang, Z.; Li, H.L.; Li, X.Y.; Yang, G.Y. An Oxalate-Functionalized Tetra-Zr^{IV}-Substituted Sandwich-Type Silicotungstate: Hydrothermal Synthesis, Structural Characterization, and Catalytic Oxidation of Thioethers. *Eur. J. Inorg. Chem.* **2019**, *2019*, 417–422. [CrossRef]

109. Lu, C.; Chen, Y.; Li, H.; Chen, L.; Zhai, C.; Zhao, J. An organic–inorganic hybrid tetra-Fe^{III} incorporated Krebs-sandwich-type tungstoantimonate decorated by pyridine carboxylic ligand. *Inorg. Chem. Commun.* **2018**, *91*, 85–90. [CrossRef]

110. Ritchie, C.; Moore, E.G.; Speldrich, M.; Kögerler, P.; Boskovic, C. Terbium polyoxometalate organic complexes: Correlation of structure with luminescence properties. *Angew. Chem. Int. Ed.* **2010**, *122*, 7868–7871. [CrossRef]

111. Lu, Y.; Xu, Y.; Wang, E.; Lü, J.; Hu, C.; Xu, L. Novel Two-Dimensional Network Constructed from Polyoxomolybdate Chains Linked through Copper−Organonitrogen Coordination Polymer Chains: Hydrothermal Synthesis and Structure of $[H_2bpy]$ $[Cu(4,4'$-bpy$)]_2[HPCuMo_{11}O_{39}]$. *Cryst. Growth Des.* **2005**, *5*, 257–260. [CrossRef]

112. Wang, J.-P.; Zhao, J.-W.; Duan, X.-Y.; Niu, J.-Y. Syntheses and Structures of One-and Two-Dimensional Organic−Inorganic Hybrid Rare Earth Derivatives Based on Monovacant Keggin-Type Polyoxotungstates. *Cryst. Growth Des.* **2006**, *6*, 507–513. [CrossRef]

113. Naruke, H.; Yamase, T. Crystal structure of K$_{18.5}$H$_{1.5}$[Ce$_3$(CO$_3$)(SbW$_9$O$_{33}$)(W$_5$O$_{18}$)$_3$]·14H$_2$O. *J. Alloys Compd.* **1998**, *268*, 100–106. [CrossRef]

114. Yamase, T.; Naruke, H.; Sasaki, Y. Crystallographic characterization of the polyoxotungstate [Eu$_3$(H$_2$O)$_3$(SbW$_9$O$_{33}$)(W$_5$O$_{18}$)$_3$]$^{18-}$ and energy transfer in its crystalline lattices. *J. Chem. Soc. Dalton Trans.* **1990**, 1687–1696. [CrossRef]

115. Ibrahim, M.; Mal, S.S.; Bassil, B.S.; Banerjee, A.; Kortz, U. Yttrium(III)-containing tungstoantimonate(III) stabilized by tetrahedral WO$_4$$^{2-}$ capping unit,[{Y(α-SbW$_9$O$_{31}$(OH)$_2$)(CH$_3$COO)(H$_2$O)}$_3$(WO$_4$)]$^{17-}$. *Inorg. Chem.* **2011**, *50*, 956–960. [CrossRef] [PubMed]

116. Mialane, P.; Dolbecq, A.; Rivière, E.; Marrot, J.; Sécheresse, F. Functionalization of Polyoxometalates by a Negatively Charged Bridging Ligand: The Dimeric [(SiW$_{11}$O$_{39}$Ln)$_2$(μ-CH$_3$COO)$_2$]$^{12-}$ (Ln= Gd^{III}, Yb^{III}) Complexes. *Eur. J. Inorg. Chem.* **2004**, *2004*, 33–36. [CrossRef]

117. Saini, M.K.; Gupta, R.; Parbhakar, S.; Mishra, A.K.; Mathur, R.; Hussain, F. Dimeric complexes of rare-earth substituted Keggin-type silicotungstates: Syntheses, crystal structure and solid state properties. *RSC Adv.* **2014**, *4*, 25357–25364. [CrossRef]

118. Hussain, F.; Degonda, A.; Sandriesser, S.; Fox, T.; Mal, S.S.; Kortz, U.; Patzke, G.R. Yttrium containing head-on complexes of silico-and germanotungstate: Synthesis, structure and solution properties. *Inorg. Chim. Acta* **2010**, *363*, 4324–4328. [CrossRef]

119. Niu, J.; Wang, K.; Chen, H.; Zhao, J.; Ma, P.; Wang, J.; Li, M.; Bai, Y.; Dang, D. Assembly chemistry between lanthanide cations and monovacant Keggin polyoxotungstates: Two types of lanthanide substituted phosphotungstates [{(α-PW$_{11}$O$_{39}$H)Ln(H$_2$O)$_3$}$_2$]$^{6-}$ and [{(α-PW$_{11}$O$_{39}$)Ln(H$_2$O)(η^2,μ-1, 1)-CH$_3$COO}$_2$]$^{10-}$. *Cryst. Growth Des.* **2009**, *9*, 4362–4372. [CrossRef]

120. Hussain, F.; Gable, R.W.; Speldrich, M.; Kögerler, P.; Boskovic, C. Polyoxotungstate-encapsulated Gd$_6$ and Yb$_{10}$ complexes. *Chem. Commun.* **2009**, *3*, 328–330. [CrossRef]

121. Chen, W.; Li, Y.; Wang, Y.; Wang, E.; Su, Z. Building block approach to nanostructures: Step-by-step assembly of large lanthanide-containing polytungstoarsenate aggregates. *Dalton Trans.* **2007**, *38*, 4293–4301. [CrossRef]

122. Arefian, M.; Mirzaei, M.; Eshtiagh-Hosseini, H.; Frontera, A. A survey of the different roles of polyoxometalates in their interaction with amino acids, peptides and proteins. *Dalton Trans.* **2017**, *46*, 6812–6829. [CrossRef]

123. Liu, J.; Yu, J.; Han, Q.; Wen, Y.; Chen, L.; Zhao, J. First quadruple-glycine bridging mono-lanthanide-substituted borotungstate hybrids. *Dalton Trans.* **2016**, *45*, 16471–16484. [CrossRef] [PubMed]

124. Li, Y.; Li, H.; Jiang, J.; Chen, L.; Zhao, J. Three Types of Distinguishing l-Alanine-Decorated and Rare-Earth-Incorporated Arsenotungstate Hybrids Prepared in a Facile One-Step Assembly Strategy. *Inorg. Chem.* **2019**, *58*, 3479–3491. [CrossRef]

125. Zhang, S.; Wang, Y.; Zhao, J.; Ma, P.; Wang, J.; Niu, J. Two types of oxalate-bridging rare-earth-substituted Keggin-type phosphotungstates {[(α-PW$_{11}$O$_9$)RE(H$_2$O)]$_2$(C$_2$O$_4$)}$^{10-}$ and {(α-x-PW$_{10}$O$_{38}$)RE$_2$(C$_2$O$_4$)(H$_2$O)$_2$}$^{3-}$. *Dalton Trans.* **2012**, *41*, 3764–3772. [CrossRef] [PubMed]

126. Mialane, P.; Dolbecq, A.; Sécheresse, F. Functionalization of polyoxometalates by carboxylato and azido ligands: Macromolecular complexes and extended compounds. *Chem. Commun.* **2006**, *33*, 3477–3485. [CrossRef] [PubMed]

127. Mialane, P.; Dolbecq, A.; Marrot, J.; Sécheresse, F. Oligomerization of Yb(III)-substituted Dawson polyoxotungstates by oxalato ligands. *Inorg. Chem. Commun.* **2005**, *8*, 740–742. [CrossRef]

128. Wang, Y.; Sun, X.; Li, S.; Ma, P.; Wang, J.; Niu, J. Synthesis and magnetic properties of tartrate-bridging rare-earth-containing polytungstoarsenate aggregates from an adaptive precursor [As$_2$W$_{19}$O$_{67}$(H$_2$O)]$^{14-}$. *Dalton Trans.* **2015**, *44*, 733–738. [CrossRef] [PubMed]

129. Ma, P.; Hu, F.; Wu, H.; Liu, X.; Wang, J.; Niu, J. Luminescent dimeric polyoxotungstate [Ho(C$_4$H$_2$O$_6$)(α-PW$_{11}$O$_{39}$)]$_2$$^{16-}$ with magnetism and reversible photochromism. *J. Lumin.* **2020**, *217*, 116760. [CrossRef]

130. Wang, Y.; Sun, X.; Li, S.; Ma, P.; Niu, J.; Wang, J. Generation of large polynuclear rare earth metal-containing organic–inorganic polytungstoarsenate aggregates. *Cryst. Growth Des.* **2015**, *15*, 2057–2063. [CrossRef]

131. Li, F.; Guo, W.; Xu, L.; Ma, L.; Wang, Y. Two dysprosium-incorporated tungstoarsenates: Synthesis, structures and magnetic properties. *Dalton Trans.* **2012**, *41*, 9220–9226. [CrossRef]

132. Ma, P.; Wan, R.; Si, Y.; Hu, F.; Wang, Y.; Niu, J.; Wang, J. Double-malate bridging tri-lanthanoid cluster encapsulated arsenotungstates: Syntheses, structures, luminescence and magnetic properties. *Dalton Trans.* **2015**, *44*, 11514–11523. [CrossRef]

133. Wu, H.; Wan, R.; Si, Y.; Ma, P.; Wang, J.; Niu, J. A helical chain-like organic–inorganic hybrid arsenotungstate with color-tunable photoluminescence. *Dalton Trans.* **2018**, *47*, 1958–1965. [CrossRef]

134. Wu, H.; Zhi, M.; Chen, H.; Singh, V.; Ma, P.; Wang, J.; Niu, J. Well-tuned white-light-emitting behaviours in multicenter-Ln polyoxometalate derivatives: A photoluminescence property and energy transfer pathway study. *Spectrochim. Acta Part A Mol. Biomol. Spectrosc.* **2019**, *223*, 117294. [CrossRef]

135. Wang, K.; Feng, S.; Ma, P. Synthesis, characterization and photoluminescence properties of a benzoic modified lanthanide-containing polyoxometalate. *Inorg. Chem. Commun.* **2019**, *108*, 107511. [CrossRef]

136. An, H.; Han, Z.; Xu, T. Three-dimensional architectures based on lanthanide-substituted double-Keggin-type polyoxometalates and lanthanide cations or lanthanide-organic complexes. *Inorg. Chem.* **2010**, *49*, 11403–11414. [CrossRef] [PubMed]

137. Ritchie, C.; Baslon, V.; Moore, E.G.; Reber, C.; Boskovic, C. Sensitization of lanthanoid luminescence by organic and inorganic ligands in lanthanoid-organic-polyoxometalates. *Inorg. Chem.* **2012**, *51*, 1142–1151. [CrossRef] [PubMed]

138. Han, Q.; Wen, Y.; Liu, J.-C.; Zhang, W.; Chen, L.-J.; Zhao, J.-W. Rare-earth-incorporated tellurotungstate hybrids functionalized by 2-picolinic acid ligands: Syntheses, structures, and properties. *Inorg. Chem.* **2017**, *56*, 13228–13240. [CrossRef]

139. Xiao, L.-N.; Zhang, T.-T.; Liu, Z.-C.; Shi, X.-M.; Zhang, H.; Yin, L.-Y.; Yao, L.-Y.; Xing, C.-C.; Cui, X.-B. Syntheses and characterizations of the first N-containing organic ligand functionalized mono-lanthanide-substituted polyoxometalates. *Inorg. Chem. Commun.* **2018**, *95*, 86–89. [CrossRef]

140. Huo, Y.; Chen, Y.-C.; Wu, S.-G.; Jia, J.-H.; Chen, W.-B.; Liu, J.-L.; Tong, M.-L. pH-controlled assembly of organophosphonate-bridged dysprosium(III) single-molecule magnets based on polyoxometalates. *Inorg. Chem.* **2018**, *57*, 6773–6777. [CrossRef]

141. Li, H.-L.; Lian, C.; Chen, L.-J.; Zhao, J.-W.; Yang, G.-Y. Two Ce3+-Substituted Selenotungstates Regulated by *N,N*-Dimethylethanolamine and Dimethylamine Hydrochloride. *Inorg. Chem.* **2019**, *58*, 8442–8450. [CrossRef]

142. Luo, J.; Zhao, J.; Yuan, J.; Li, Y.; Chen, L.; Ma, P.; Wang, J.; Niu, J. An organic–inorganic hybrid 1-D double-chain copper–yttrium heterometallic silicotungstate [Cu(dap)$_2$(H$_2$O)]$_2${Cu(dap)$_2$[α-H$_2$SiW$_{11}$O$_{39}$Y(H$_2$O)$_2$]$_2$}·10H$_2$O. *Inorg. Chem. Commun.* **2013**, *27*, 13–17. [CrossRef]

143. Wang, J.-P.; Yan, Q.-X.; Du, X.-D.; Niu, J.-Y. Hydrothermal Synthesis and Crystal Structure of One Rare Earth Substituted Keggin-Type Germanotungstate [Cu(en)$_2$]$_2$[Cu(en)$_2$(H$_2$O)]$_2$H$_3${[Cu(en)$_2$]$_2$[Na$_2$(H$_2$O)$_{1.75}$][K(H$_2$O)$_3$][Dy$_2$(H$_2$O)$_2$(GeW$_{11}$O$_{39}$)$_3$]}·6H$_2$O. *J. Clust. Sci.* **2008**, *19*, 491–498. [CrossRef]

144. Compain, J.-D.; Mialane, P.; Dolbecq, A.; Mbomekalle, I.M.; Marrot, J.; Secheresse, F.; Duboc, C.; Riviere, E. Structural, magnetic, EPR, and electrochemical characterizations of a spin-frustrated trinuclear Cr^{III} polyoxometalate and study of its reactivity with lanthanum cations. *Inorg. Chem.* **2010**, *49*, 2851–2858. [CrossRef]

145. Wang, J.-P.; Duan, X.-Y.; Du, X.-D.; Niu, J.-Y. Novel rare earth germanotungstates and organic hybrid derivatives: Synthesis and structures of M/[α-GeW$_{11}$O$_{39}$](M = Nd, Sm, Y, Yb) and Sm/[α-GeW$_{11}$O$_{39}$](DMSO). *Cryst. Growth Des.* **2006**, *6*, 2266–2270. [CrossRef]

146. Wang, J.P.; Yan, Q.X.; Du, X.D.; Niu, J.Y. Synthesis, Crystal Structure and Characterization of Two Rare Earth Substituted Keggin-Type Germanotungstates. *Chin. J. Chem.* **2008**, *26*, 1239–1243. [CrossRef]

147. Reinoso, S.; Galán-Mascarós, J.R. Heterometallic 3d− 4f polyoxometalate derived from the weakley-type dimeric structure. *Inorg. Chem.* **2010**, *49*, 377–379. [CrossRef] [PubMed]

148. Kortz, U.; Nellutla, S.; Stowe, A.C.; Dalal, N.S.; Rauwald, U.; Danquah, W.; Ravot, D. Sandwich-type germanotungstates: Structure and magnetic properties of the dimeric polyoxoanions [M$_4$(H$_2$O)$_2$(GeW$_9$O$_{34}$)$_2$]$^{12-}$ (M = Mn^{2+}, Cu^{2+}, Zn^{2+}, Cd^{2+}). *Inorg. Chem.* **2004**, *43*, 2308–2317. [CrossRef] [PubMed]

149. Nohra, B.; Mialane, P.; Dolbecq, A.; Rivière, E.; Marrot, J.; Sécheresse, F. Heterometallic 3d–4f cubane clusters inserted in polyoxometalate matrices. *Chem. Commun.* **2009**, *19*, 2703–2705. [CrossRef] [PubMed]

150. Wu, H.-H.; Yao, S.; Zhang, Z.-M.; Li, Y.-G.; Song, Y.; Liu, Z.-J.; Han, X.-B.; Wang, E.-B. Heterometallic appended {MMn III 4} cubanes encapsulated by lacunary polytungstate ligands. *Dalton Trans.* **2013**, *42*, 342–346. [CrossRef]

151. Chen, Y.-Z.; Liu, Z.-J.; Zhang, Z.-M.; Zhou, H.-Y.; Zheng, X.-T.; Wang, E.-B. Systematic assembly of {LnMnIII4} appended cubanes with inorganic polyoxometalate ligands and their electrocatalytic property. *Inorg. Chem. Commun.* **2014**, *46*, 155–158. [CrossRef]

152. Cai, J.; Zheng, X.-Y.; Xie, J.; Yan, Z.-H.; Kong, X.-J.; Ren, Y.-P.; Long, L.-S.; Zheng, L.-S. Anion-dependent assembly of heterometallic 3d–4f clusters based on a lacunary polyoxometalate. *Inorg. Chem.* **2017**, *56*, 8439–8445. [CrossRef]

153. Du, D.-Y.; Qin, J.-S.; Li, S.-L.; Wang, X.-L.; Yang, G.-S.; Li, Y.-G.; Shao, K.-Z.; Su, Z.-M. A series of inorganic–organic hybrid compounds constructed from bis(undecatungstophosphate) lanthanates and copper-organic units. *Inorg. Chim. Acta* **2010**, *363*, 3823–3831. [CrossRef]

154. Li, B.; Zhao, J.-W.; Zheng, S.-T.; Yang, G.-Y. Two Novel 1-D Organic–Inorganic Composite Phosphotungstates Constructed from [Ln(α-PW$_{11}$O$_{39}$)$_2$]$^{11-}$ Units and [Cu(en)$_2$]$^{2+}$ Bridges (Ln = Ce^{III}/Er^{III}). *J. Clust. Sci.* **2009**, *20*, 503–513. [CrossRef]

155. Du, D.-Y.; Qin, J.-S.; Yuan, G.; Lan, Y.-Q.; Wang, X.-L.; Shao, K.-Z.; Su, Z.-M. Building block approach to a series of substituted Keggin-type inorganic–organic hybrids. *Solid State Sci.* **2011**, *13*, 1115–1121. [CrossRef]

156. Zhao, J.; Shi, D.; Chen, L.; Ma, P.; Wang, J.; Zhang, J.; Niu, J. Tetrahedral polyoxometalate nanoclusters with tetrameric rare-earth cores and germanotungstate vertexes. *Cryst. Growth Des.* **2013**, *13*, 4368–4377. [CrossRef]

157. Shi, D.-Y.; Zhao, J.-W.; Chen, L.-J.; Ma, P.-T.; Wang, J.-P.; Niu, J.-Y. Four types of 1D or 2D organic–inorganic hybrids assembled by arsenotungstates and Cu II–Ln III/IV heterometals. *CrystEngComm* **2012**, *14*, 3108–3119. [CrossRef]

158. Chen, L.; Shi, D.; Wang, Y.; Cheng, H.; Geng, Z.; Zhao, J.; Ma, P.; Niu, J. Two 3d–4f heterometallic monovacant Keggin phosphotungstate derivatives. *J. Coord. Chem.* **2011**, *64*, 400–412. [CrossRef]

159. Shi, D.; Chen, L.; Zhao, J.; Wang, Y.; Ma, P.; Niu, J. Two novel 2D organic–inorganic hybrid lacunary Keggin phosphotungstate 3d–4f heterometallic derivatives:[Cu(en)$_2$]$_2$H$_6$[Ce(α-PW$_{11}$O$_{39}$)$_2$]·8H$_2$O and [Cu(dap)$_2$(H$_2$O)][Cu(dap)$_2$]$_{4.5}$[Dy (α-PW$_{11}$O$_{39}$)$_2$]·4H$_2$O. *Inorg. Chem. Commun.* **2011**, *14*, 324–329. [CrossRef]

160. Zhang, S.; Zhao, J.; Ma, P.; Chen, H.; Niu, J.; Wang, J. Organic–Inorganic Hybrids Based on Monovacant Keggin-type Silicotungstates and 3d-4f Heterometals. *Cryst. Growth Des.* **2012**, *12*, 1263–1272. [CrossRef]

161. Zhao, J.; Shi, D.; Chen, L.; Li, Y.; Ma, P.; Wang, J.; Niu, J. Novel polyoxometalate hybrids consisting of copper–lanthanide heterometallic/lanthanide germanotungstate fragments. *Dalton Trans.* **2012**, *41*, 10740–10751. [CrossRef] [PubMed]

162. Wang, W.-D.; Li, X.-X.; Fang, W.-H.; Yang, G.-Y. Hydrothermal synthesis and structural characterization of a new Keggin-type tungstogermanate containing heterometallic 3d–4f cubane clusters. *J. Clust. Sci.* **2011**, *22*, 87–95. [CrossRef]

163. Zhang, J.; Li, J.; Li, L.; Zhao, H.; Ma, P.; Zhao, J.; Chen, L. Syntheses, structures, spectroscopic and electrochemical properties of two 1D organic–inorganic Cu^{II}–Ln^{III} heterometallic germanotungstates. *Spectrochim. Acta Part A Mol. Biomol. Spectrosc.* **2013**, *114*, 360–367. [CrossRef]

164. Han, Q.; Wen, Y.; Liu, J.; Chen, L.; Zhao, J. Synthesis, structure and electrochemical properties of an inorganic–organic hybrid Cu^{II}Ce^{III} heterometallic germanotungstate. *Inorg. Chem. Commun.* **2016**, *71*, 54–60. [CrossRef]

165. Li, Y.; Tian, S.; Li, Y.; Zhao, J.; Ma, P.; Chen, L. Two 2D Cu–Ln heterometallic polyoxometalate aggregates constructed from bis (undecatungstophosphate) lanthanate units and copper-complex bridges. *Inorg. Chim. Acta* **2013**, *405*, 105–110. [CrossRef]

166. Zhao, H.-Y.; Yang, B.-F.; Yang, G.-Y. Two new 2D organic–inorganic hybrids assembled by lanthanide-substituted polyoxotungstate dimers and copper–complex linkers. *Inorg. Chem. Commun.* **2017**, *84*, 212–216. [CrossRef]

167. Shang, S.; Zhao, J.; Chen, L.; Li, Y.; Zhang, J.; Li, Y.; Niu, J. 2-D and 3-D phosphotungstate-based TM–Ln heterometallic derivatives constructed from dimeric [Ln(α-PW$_{11}$O$_{39}$)$_2$]$^{11-}$ fragments and copper-organic complex linkers. *J. Solid State Chem.* **2012**, *196*, 29–39. [CrossRef]

168. Luo, J.; Leng, C.; Chen, L.; Yuan, J.; Li, H.; Zhao, J. Three 3D organic–inorganic hybrid heterometallic polyoxotungstates assembled from 1: 2-type [Ln(α-SiW$_{11}$O$_{39}$)$_2$]$^{13-}$ silicotungstates and [Cu(dap)$_2$]$^{2+}$ linkers. *Synth. Met.* **2012**, *162*, 1558–1565. [CrossRef]

169. Yao, S.; Yan, J.H.; Duan, H.; Zhang, Z.M.; Li, Y.G.; Han, X.B.; Shen, J.Q.; Fu, H.; Wang, E.B. Integration of Ln-Sandwich POMs into Molecular Porous Systems Leading to Self-Assembly of Metal–POM Framework Materials. *Eur. J. Inorg. Chem.* **2013**, *2013*, 4770–4774. [CrossRef]

170. Zhao, J.-W.; Li, Y.-Z.; Ji, F.; Yuan, J.; Chen, L.-J.; Yang, G.-Y. Syntheses, structures and electrochemical properties of a class of 1-D double chain polyoxotungstate hybrids [H$_2$dap][Cu(dap)$_2$]$_{0.5}$[Cu(dap)$_2$(H$_2$O)][Ln(H$_2$O)$_3$(α-GeW$_{11}$O$_{39}$)]·3H$_2$O. *Dalton Trans.* **2014**, *43*, 5694–5706. [CrossRef]

171. Zhao, J.; Luo, J.; Chen, L.; Yuan, J.; Li, H.; Ma, P.; Wang, J.; Niu, J. Novel 1-D double-chain organic–inorganic hybrid polyoxo-tungstates constructed from dimeric copper–lanthanide heterometallic silicotungstate units. *CrystEngComm* **2012**, *14*, 7981–7993. [CrossRef]

172. Wu, S.-Y.; Wang, Y.-J.; Jing, J.-X.; Li, X.-X.; Sun, Y.-Q.; Zheng, S.-T. Two organic–inorganic hybrid polyoxotungstogermanates containing organic ligand chelated Fe–Dy heterometallic clusters and frequency dependent magnetic properties. *Inorg. Chem. Front.* **2020**, *7*, 498–504. [CrossRef]

173. Jingping, W.; Wei, W.; Qingxia, Y.; Jingyang, N. Synthesis and crystal structure of a novel double 1:11 series arsenotungstate: [Cu^I(phen)$_2$]$_5$H$_6$[Sm(AsW$_{11}$O$_{39}$)$_2$]·6H$_2$O. *J. Rare Earths* **2008**, *26*, 638–642.

174. Zhou, W.; Liu, P.; Zheng, Y.; Peng, J. Bifunctional electro-catalysts stemmed from Ln-Substituted monovacant/saturated Keggin polyoxotungstates and cu-terpyridine chlorides. *Catal. Surv. Asia* **2018**, *22*, 136–145. [CrossRef]

175. Zhou, W.; Zhang, Z.; Peng, J.; Wang, X.; Shi, Z.; Li, G. A series of hybrids with a framework constructed from {–SiW$_{11}$–Ln–SiW$_{11}$–}$_n$ chains and {Cu/bimpy} ribbons. *CrystEngComm* **2014**, *16*, 10893–10901. [CrossRef]

176. Kortz, U.; Savelieff, M.G.; Bassil, B.S.; Keita, B.; Nadjo, L. Synthesis and characterization of iron (III)-substituted, dimeric polyoxotungstates,[Fe$_4$(H$_2$O)$_{10}$(β-XW$_9$O$_{33}$)$_2$]$^{n-}$(n = 6, X= As^{III}, Sb^{III}; n= 4, X = Se^{IV}, Te^{IV}). *Inorg. Chem.* **2002**, *41*, 783–789. [CrossRef]

177. Zhao, J.-W.; Cao, J.; Li, Y.-Z.; Zhang, J.; Chen, L.-J. First tungstoantimonate-based transition-metal–lanthanide heterometallic hybrids functionalized by amino acid ligands. *Cryst. Growth Des.* **2014**, *14*, 6217–6229. [CrossRef]

178. Chen, L.; Zhang, F.; Ma, X.; Luo, J.; Zhao, J. Two types of novel tetra-iron substituted sandwich-type arsenotungastates with supporting lanthanide pendants. *Dalton Trans.* **2015**, *44*, 12598–12612. [CrossRef]

179. Chen, Y.; Sun, L.; Chang, S.; Chen, L.; Zhao, J. Synergistic effect between different coordination geometries of lanthanides and various coordination modes of 2-picolinic acid ligands tuning three types of rare 3d–4f heterometallic tungstoantimonates. *Inorg. Chem.* **2018**, *57*, 15079–15092. [CrossRef]

180. Yao, S.; Zhang, Z.; Li, Y.; Lu, Y.; Wang, E.; Su, Z. Two heterometallic aggregates constructed from the {P$_2$W$_{12}$}-based trimeric polyoxotungstates and 3d-4f heterometals. *Cryst. Growth Des.* **2010**, *10*, 135–139. [CrossRef]

181. Zhang, Z.-M.; Li, Y.-G.; Yao, S.; Wang, E.-B. Hexameric polyoxometalates decorated by six 3d–4f heterometallic clusters. *Dalton Trans.* **2011**, *40*, 6475–6479. [CrossRef]

182. Zhao, H.-Y.; Zhao, H.-Y.; Yang, B.-F.; He, H.; Yang, B.-F. Novel three-dimensional organic-inorganic heterometallic hybrid built by sandwich-type tetra-Mn-substituted germanotungstates through mixed 3d and 4f metal linkers. *Cryst. Growth Des.* **2013**, *13*, 5169–5174. [CrossRef]

183. Xue, H.; Zhang, Z.; Pan, R.; Yang, B.-F.; Liu, H.-S.; Yang, G.-Y. Supramolecular nanotubes constructed from 3d–4f heterometallic sandwiched polyoxotungstate dimers. *CrystEngComm* **2016**, *18*, 4643–4650. [CrossRef]

184. Sato, R.; Suzuki, K.; Minato, T.; Yamaguchi, K.; Mizuno, N. Sequential Synthesis of 3d–3d′–4f Heterometallic Heptanuclear Clusters in between Lacunary Polyoxometalates. *Inorg. Chem.* **2016**, *55*, 2023–2029. [CrossRef]

185. Du, D.; Qin, J.; Li, S.; Lan, Y.; Wang, X.; Su, Z. 3d–4f Heterometallic complexes for the construction of POM-based inorganic–organic hybrid compounds: From nanoclusters to one-dimensional ladder-like chains. *Aust. J. Chem.* **2010**, *63*, 1389–1395. [CrossRef]

186. Zhao, H.-Y.; Zhao, J.-W.; Yang, B.-F.; Wei, Q.; Yang, G.-Y. Two Organic–Inorganic Hybrids Assembled by Carboxylate-Bridging Lanthanide-Substituted Polyoxometalate Dimers with Copper–ethylendiamine Cations. *J. Clust. Sci.* **2014**, *25*, 667–680. [CrossRef]

187. Zhao, H.-Y.; Zhao, J.-W.; Yang, B.-F.; He, H.; Yang, G.-Y. Organic-inorganic hybrids based on monovacant Keggin-type polyoxo-tungstates and 3d–4f heterometals. *CrystEngComm* **2013**, *15*, 8186–8194. [CrossRef]

188. Sun, L.; Liu, Y.; Wang, X.; Li, H.; Luo, J.; Chen, L.; Zhao, J. Syntheses, structures and properties of a series of inorganic–organic hybrid copper–lanthanide heterometal comprising germanotungstates with mixed ligands. *Synth. Met.* **2016**, *217*, 256–265. [CrossRef]

189. Zhao, H.-Y.; Zhao, J.-W.; Yang, B.-F.; He, H.; Yang, G.-Y. Novel organic–inorganic hybrid one-dimensional chain assembled by oxalate-bridging terbium-substituted phosphotungstate dimers and dinuclear copper(II)–oxalate clusters. *CrystEngComm* **2013**, *15*, 5209–5213. [CrossRef]

190. Zhang, Z.-H.; Zhang, Z.; Yang, B.-F.; He, H.; Yang, G.-Y. Two novel 2D organic–inorganic hybrid silicotungstates assembled by {$Cu_2Ln_2(ox)(SiW_{11})_2$} dimers and [Cu(en)(ox)]/[Cu(en)$_2$] linkers. *Inorg. Chem. Commun.* **2016**, *63*, 65–68. [CrossRef]

191. Wang, F.-Q.; Zheng, X.-J.; Wan, Y.-H.; Wang, K.-Z.; Jin, L.-P. Architecture of zero-, one-, two-and three-dimensional structures based on metal ions and pyrazine-2, 6-dicarboxylic acid. *Polyhedron* **2008**, *27*, 717–726. [CrossRef]

192. Zhang, S.; Zhao, J.; Ma, P.; Niu, J.; Wang, J. Rare-Earth–Transition-Metal Organic–Inorganic Hybrids Based on Keggin-type Polyoxometalates and Pyrazine-2, 3-dicarboxylate. *Chem.–Asian J.* **2012**, *7*, 966–974. [CrossRef] [PubMed]

193. Sun, P.; Ma, F.; Liu, S. Inorganic-organic hybrids constructed of bis (undecatungstogermanate) lanthanates polyoxoanions and oxalate-bridged dinuclear copper complexes and their magnetic properties. *Chin. Sci. Bull.* **2011**, *56*, 2331–2336. [CrossRef]

194. Gupta, R.; Parbhakar, S.; Behera, J.N.; Hussain, F. Sandwich type organic-inorganic hybrid of 3d–4f heterometallic containing germanotungstates [{$Cu_2(1, 10$-phen)$_2(\mu$-$CH_3COO)_2$}Ln(α-$GeW_{11}O_{39})_2$]$^{11-}$: Syntheses, crystal structures, magnetic and photoluminescence properties. *Inorg. Chem. Commun.* **2016**, *74*, 72–78. [CrossRef]

195. Cao, J.; Liu, S.; Cao, R.; Xie, L.; Ren, Y.; Gao, C.; Xu, L. Organic–inorganic hybrids assembled by bis (undecatungstophosphate) lanthanates and dinuclear copper(II)–oxalate complexes. *Dalton Trans.* **2008**, *1*, 115–120. [CrossRef]

196. Niu, J.; Zhang, S.; Chen, H.; Zhao, J.; Ma, P.; Wang, J. 1-D, 2-D, and 3-D organic–inorganic hybrids assembled from Keggin-type polyoxometalates and 3d-4f heterometals. *Cryst. Growth Des.* **2011**, *11*, 3769–3777. [CrossRef]

197. Martín-Caballero, J.; Artetxe, B.; Reinoso, S.; San Felices, L.; Vitoria, P.; Larrañaga, A.; Vilas, J.L.; Gutiérrez-Zorrilla, J.M. Thermostructural behavior in a series of lanthanide-containing polyoxotungstate hybrids with copper(II) complexes of the tetraazamacrocycle cyclam: A single-crystal-to-single-crystal transformation study. *Inorg. Chem.* **2019**, *58*, 4365–4375. [CrossRef]

198. Han, Q.; Liu, J.-C.; Wen, Y.; Chen, L.-J.; Zhao, J.-W.; Yang, G.-Y. Tellurotungstate-based organotin–rare-earth heterometallic hybrids with four organic components. *Inorg. Chem.* **2017**, *56*, 7257–7269. [CrossRef] [PubMed]

199. Liu, J.-C.; Zhao, J.-W.; Song, Y.-F. 1-D Chain Tungstotellurate Hybrids Constructed from Organic-Ligand-Connecting Iron–Lanthanide Heterometal Encapsulated Tetrameric Polyoxotungstate Units. *Inorg. Chem.* **2019**, *58*, 9706–9712. [CrossRef] [PubMed]